The Effect of Solar Ultraviolet Induced Activation of Constitutive Nitric Oxide Synthase on Primary Fibroblast Cells

Thesis by Christina Ioanna Athans

Honors Tutorial College Biological Sciences

Thesis Advisors: Dr. Veronica Bahamondes Lorca

And Dr. Shiyong Wu

Director of Studies: Dr. Soichi Tanda

Table of Contents

Abstract

The skin is the largest organ of the human body and has highly complex functions in the body. It serves an important role in protecting against chemical and physical factors, such as ultraviolet (UV) radiation from the sun. The UV radiation emitted from the sun is composed of UVA, UVB, and UVC wavelengths ranging from 200 nm to 400 nm. UVA is the portion having the longest wavelength (320 nm - 400 nm) and has the deepest penetration into the skin. UVB (280 nm - 320 nm) penetrates the skin only into the superficial layers. UVC (200 nm - 280 nm) is blocked by the atmosphere and does not reach the Earth's surface. When our skin is exposed to solar UV (sUV) radiation, many immediate and delayed reactions occur, having both positive and negative effects on the body. One particular effect of sUV exposure is the increase in reactive oxygen and nitrogen species from the activation of the nitric oxide synthases (NOSs). UVB induces rapid activation of the constitutive NOS (cNOSs), including endothelial NOS (eNOS) and neuronal NOS (nNOS). Upon activation, cNOSs produce nitric oxide (NO·) or superoxide (O_2·-), the two molecules that can react rapidly to form peroxynitrite (ONOO-). Previously we showed that cNOSs are involved in the apoptotic signaling pathway via translational regulation of IκB expression and NF-κB activation in human keratinocyte HaCaT cells post-UVB exposure. To further study the role of sUV-induced activation of cNOS in skin cells, DNA damage and repair, inflammation, and photoaging were analyzed. An *in vitro* model was established using fibroblasts isolated from cNOS knock-out mice. In this study, we provide evidence that cNOSs are also involved in DNA damage repair post-sUV, the processing of MMP2, and the production of IL6.

Acknowledgements

Firstly, I would like to thank the Honors Tutorial College for the opportunity to engage in undergraduate research, and for pushing me to pursue a thesis project. This endeavor would not have been possible without the support of my academic and research advisors, so I owe a huge thank you to them. Thank you to Dr. Tanda, who has been an invaluable mentor to me in my undergraduate career as my academic advisor. Thank you to Dr. Wu, who has provided me countless opportunities to grow as a scientist and has given me the opportunity to be a collaborator in the field. And thank you to Dr. Bahamondes Lorca, or Veronica, as I know her by, who has been the single most influential person in my experience with research and to this thesis project. I would like to also acknowledge the other undergraduate and graduate researchers in Dr. Wu's lab, and all staff at Edison Biotechnology Institute, thank you for the support. Thank you to all my other professors and mentors along the way, who have shaped me into the person I am today.

Thank you to my peers who have gone through their own journeys and been by my side for our time at Ohio University. The support of my fellow HTC students has made all the difference. And finally, thank you to my family. To my sister for always being by my side, to my parents for supporting me through everything, and to my Yiayia for always encouraging me every step of the way.

1. Introduction

Sunlight and ultraviolet (UV) radiation are crucial to life on earth, playing key roles in processes such as the synthesis of vitamin D, which is critical for overall health, regulation of immune response, which is beneficial in the treatment of autoimmune disorders, as well as the treatment of various inflammatory diseases such as atherosclerosis (Englesen, 2010), (Sasaki et at., 2017), (Bernard et al., n.d.). Despite the necessity of UV radiation and the known benefits, overexposure leads to the promotion of detrimental effects within the body. As seen in figure 1, the effects of solar UV (sUV) exposure are classified as immediate, short-term, and long-term. Immediate effects are mostly harmless. However, the delayed and long-term effects negatively impact human health (Juzeniene et al., 2011). Our body's largest organ and the first line of defense against UV radiation is our skin. Elevated absorption of excess UV radiation by our skin leads to increased inflammation, premature photoaging, oxidative stress, and ultimately skin cancer, which are preventable when the correct precautions are taken (Valacchi et al., n.d.).

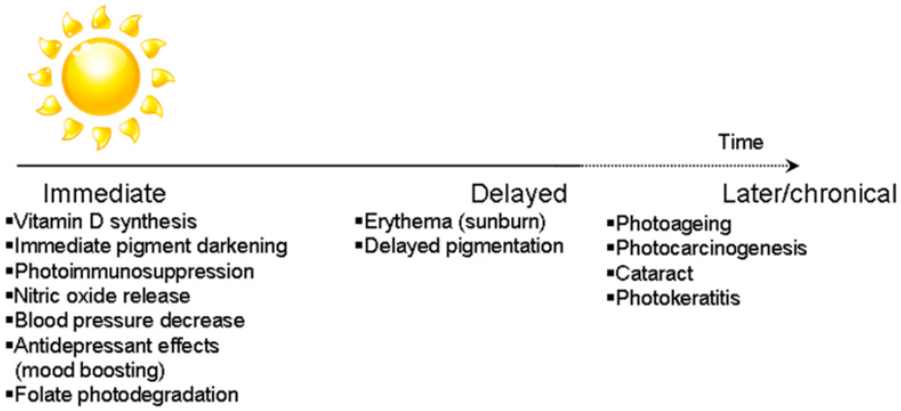

Figure 1 Immediate, short-term, and long-term effects of solar UV exposure. Immediate effects are mostly harmless, while long-term effects have detrimental impacts on health. Note. Reprinted from "Solar radiation and human health", by Juzeniene et al., 2011, Reports on Progress in Physics, 74(6), p.5

1.1 Ultraviolet Light

To understand the effects of UV exposure, we must understand the components of the most common UV source - the sun. sUV radiation is made up of three distinct UV spectrums - UVA, UVB, and UVC. Figure 2 shows the components of sUV as well as the depth of penetration in the skin (D'orazio et al., 2013). The various components of sUV radiation have distinct effects on the body. UVC radiation is the range of light falling between 200 nm and 280 nm. UVC is the most lethal form of UV radiation and is most harmful to living organisms because DNA absorbs UV radiation most efficiently at 260 nm (Juzeniene et al., 2011). Luckily, damaging UVC radiation from the sun is absorbed by Earth's ozone layer, mitigating all damage that would be caused if it were to reach Earth's surface.

The 280 nm to 320 nm range is classified as UVB, while the wavelength range between 320 nm and 400 nm corresponds to UVA. UVA makes up roughly 95% of the solar UV radiation that reaches the Earth's surface, while the remaining 5% is UVB (Anderson et al., n.d.). As the wavelength of UV radiation increases, so does the depth of penetration; UVB can penetrate the skin only through the epidermis and superficial dermis. Unlike UVB, UVA interacts with both the epidermis and deep into the dermis (Bahamondes-Lorca et al., 2021). UVB causes damage to the skin that results in sunburn, inflammation, skin aging (photoaging), and possibly cancer (Yamaba et al., 2016). The penetration into the dermal layer of our skin by UVA causes damage resulting in irritation, inflammation, and specifically photoaging (de Jager et al., 2017). This is due to the interactions UVA wavelengths have with dermal cells such as fibroblasts, which play

an important role in the formation of connective tissue and the maintenance of the extracellular matrix of the skin.

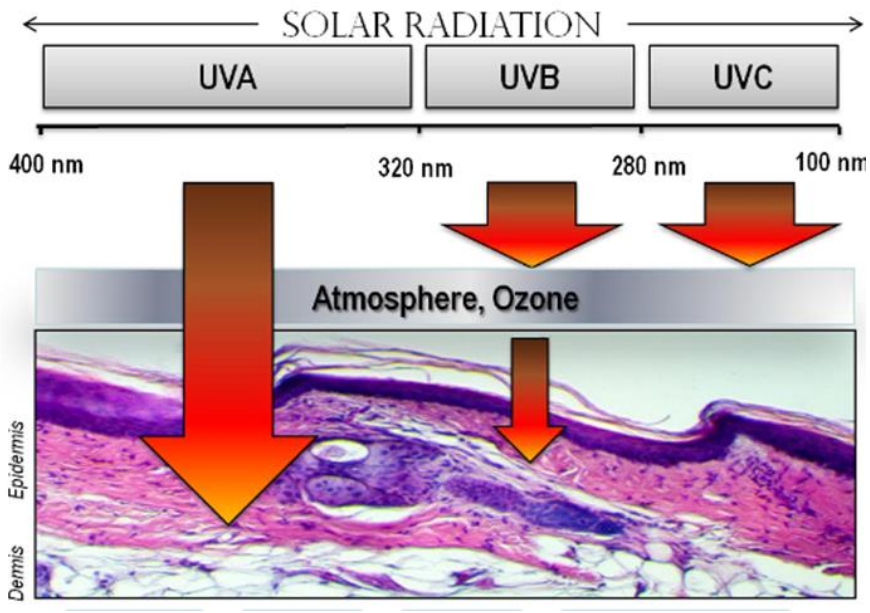

Figure 2 Depth of penetration of solar UV components, UVA, UVB, and UV. Note. Modified from "UV Radiation and the Skin, by D'orazio et al., 2013, International Journal of Molecular Sciences, 14, p.12227. Article published under an open access Creative Common CC By license.

1.2 Skin

As previously stated, the skin is the largest organ functioning as a barrier that protects against elements such as UV radiation from the sun and harmful bacteria. Other functions of the skin include regulating body temperature and enabling touch and sensation (Cleveland Clinic). In addition to these basic functions of the skin, each layer of skin has specialized functions, based on the components in the prospective layers.

The most superficial portion of the skin is the epidermis, which is the most protective region, as it is the body's first barrier to the outside elements. The epidermis has four to five layers based on the location of the body. From superficial to deep, these layers include the stratum corneum, stratum lucidum (which is only present in thick skin), stratum granulosum, stratum spinosum, and stratum basale (Murphey et al., 2022).

The stratum corneum consists of corneocytes, which are anucleated keratinocytes filled with keratin proteins produced by the keratinocytes found in the stratum spinosum layer (Murphey et al., 2022). Corneocytes are matured keratinocyte cells in the final stage of cellular differentiation. They do not contain a nucleus or functioning organelles and contribute to the waterproofing and protective functions of the skin. Corneocytes are "dead" skin cells that do not proliferate further and are sloughed off as new cells are produced (Murphy et al., 2022). The stratum lucidum is a thin, translucent layer which is only found in the thick skin on the lips, palms, soles, and digits (these areas of the body do not grow hair). It is also made of keratinocyte derivatives containing the clear protein, eleidin (Murphey et al., 2022). Deep to the stratum lucidum is the stratum granulosum, a layer which is characterized by cells with keratohyalin and lamellar granules. Keratohyalin granules contain keratin precursors while lamellar granules are filled with glycolipids. The next deepest layer is the stratum spinosum, which gets its name from the "spiny" appearance of the keratinocytes located in this layer observed after the histological staining process. This appearance is due to structures known as desmosomes, which are cell-junction complexes. Desmosomes present in the stratum spinosum act as cell connectors and

strengthen the intercellular bonds (Ramadon et al., 2021). Langerhans cells, which are dendritic immune cells in the skin, are also found in the stratum spinosum (Yousef et al., 2022).

The deepest layer of the epidermis is the stratum basale, which connects the epidermis to the dermis. The main cells of this layer are primary basal cells, which differentiate to form keratinocytes. The keratinocytes made in the stratum basale push up and travel to the superficial layers of skin, and replace old cells in a constant cycle. Other specialized cells found in the stratum basale are melanocytes and Merkel cells (Ramadon et al., 2021). Melanocytes are skin cells that produce melanin to pigment the skin. Melanocytes are stimulated in response to excess sunlight in order to create more melanin, which protects the skin from sun damage. Merkel cells are sensory cells that receive touch/pressure input (Ramadon et al., 2021).

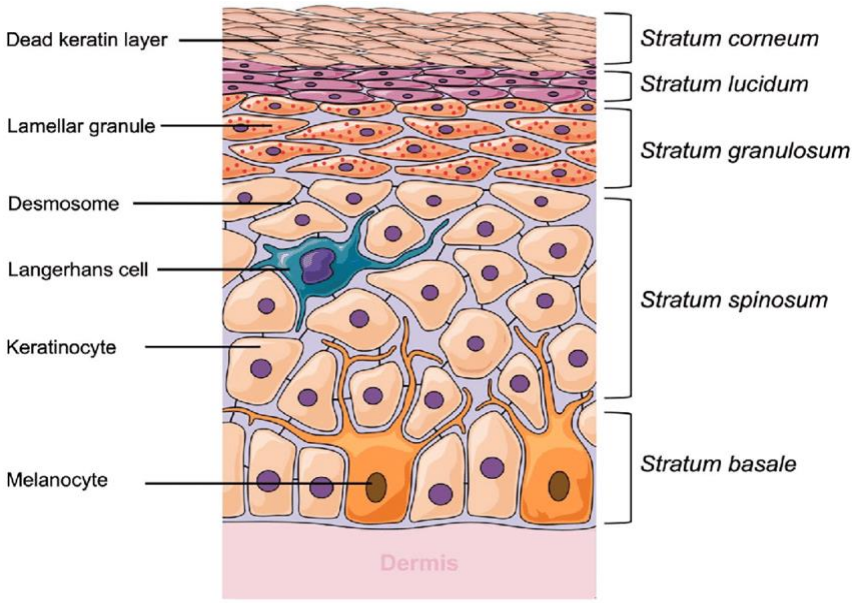

Figure 3 Visual representation of the five layers of the epidermis with correlating cells. "Enhancement strategies for transdermal drug delivery systems: current trends and applications" by Ramadon et al., January 2021. Drug Delivery and Translational Research. 12. 10.1007/s13346-021-00909-6. Available via license: Creative Commons Attribution 4.0 International.

Below the epidermis is the dermis, which is a highly vascular layer divided into the superficial papillary region, composed of loose connective tissue, and the deep reticular layer, which is composed of dense connective tissue. The principal components of the dermis are collagen fibers and elastic fibers suspended in the extracellular matrix (Brown & Krishnamurthy 2022). Collagen fibers consist of a bundle of collagen fibrils formed by collagen proteins, whereas elastic fibers are composed mainly of elastin and fibrillin-rich microfibrils. Collagen fibers in the skin provide strength and durability while elastic fibers due to the presence of elastin contribute to the flexibility and stretchability of the skin. In addition to these components, many secretory glands and sensory receptors are found in the dermis, including sebaceous glands, sweat glands, free nerve endings, touch and pressure receptors, and blood vessels. An array of cell types are found in the dermis, including adipocytes, or fat cells, macrophages, mast cells, Schwann cells, stem cells, and fibroblasts. Fibroblasts play an important role in the integrity of the skin, as they are responsible for the production of both collagen and elastin fibers, as well as other extracellular matrix compounds (Brown & Krishnamurthy 2022).

The deepest layer of the skin is the subcutaneous layer, or hypodermis. This layer of the skin is a vascular layer mainly composed of adipocytes. The hypodermis serves as a cushioning layer which protects the muscular and skeletal systems that lie beneath the skin. An important role of the hypodermis is temperature regulation, as the adipose in this layer helps to conserve body heat (Yousef et al., 2022).

1.3 Role of Fibroblasts in the Skin

Fibroblasts synthesize and secrete collagen, an abundant protein present in the extracellular matrix (ECM), which makes them an important factor for the maintenance of connective tissue. In addition to the secretion of collagen, which is the most abundant protein in the body, other ECM- related proteins such as proteoglycans, fibronectins, laminins, glycosaminoglycans, and matrix metalloproteinases are produced by them. Fibroblasts not only provide proteins necessary for the formation of the connective tissue of the skin, but they also supply the proteins required for the support and connection between internal organs, which in addition play a vital role in cell signaling for other organs in the body. In the skin, fibroblasts are a dermal cell type, meaning they are located in the layer between the epidermis (most superficial skin layer) and hypodermis (deepest skin layer). Because the dermis is not a homogenous layer, fibroblasts express different varieties and quantities of proteins depending on their position, as shown in figure 4 (Tracy et al., 2014).

It is well known that the general function of fibroblast is the maintenance of ECM and the synthesis of collagen. For maintaining the ECM, fibroblasts secrete matrix metalloproteinases (MMPs), which are a family of protein proteases that degrade collagen and other ECM proteins. The degradation of collagen in the skin can lead to the appearance of wrinkles and aging of the skin. Because of this function, MMPs play a role in inflammation and aging. In the human skin, 19 MMPs are described and 3 are known to have increased expression after UV exposure (MMP-1, MMP-3, and MMP-9). Fibroblasts also secrete tissue inhibitors of metalloproteinases or TIMPs, which deactivate MMPs. TIMPs then help in the maintenance of the correct amount

of active MMPs in the ECM (Quan et al., 2009). As with the MMPs, UV irradiation also induces an increased expression of the TIMPs proteins (Quan et al., 2009).

Fibroblasts are also important in the cellular signaling processes that take place in the skin. Fibroblasts communicate with other cells within the skin, including keratinocytes in the epidermis, vascular and neural cells in the dermis, and cells from the hematopoietic lineage, such as dendritic cells and leukocytes via paracrine and autocrine signaling. These cellular interactions impact the regulation of processes such as cellular proliferation, morphogenesis, wound healing, skin response to UV, and cancer. An example of these interactions is that of fibroblast growth factor 2 (FGF2). FGF2 is secreted by normal fibroblasts and keratinocytes, as well as UVB-irradiated keratinocytes. Depending on the tissue's environment and the conditions for which FGF2 is secreted, melanocytes are activated or transformed in response to FGF2. This response is important for the development of skin cancer within the melanocytes (known as melanoma) (Czy et al., 2019). FGF2 is also reported to be overexpressed in basal cell carcinoma (BCC), a skin cancer that affects the basal cells of the epidermis (Czy et al., 2019). As mentioned by Sorrell and Caplan, other fibroblast secretions that play a role in proliferation include granulocyte-macrophage colony-stimulating factor (GM-CSF), FGF-10 (also known as KGF-2), parathyroid-hormone-related protein, hepatocyte growth factor/scatter factor (HGF/SF), epidermal growth factor (EGF) and interleukin 6 (IL-6) (Sorrell & Caplan, 2004).

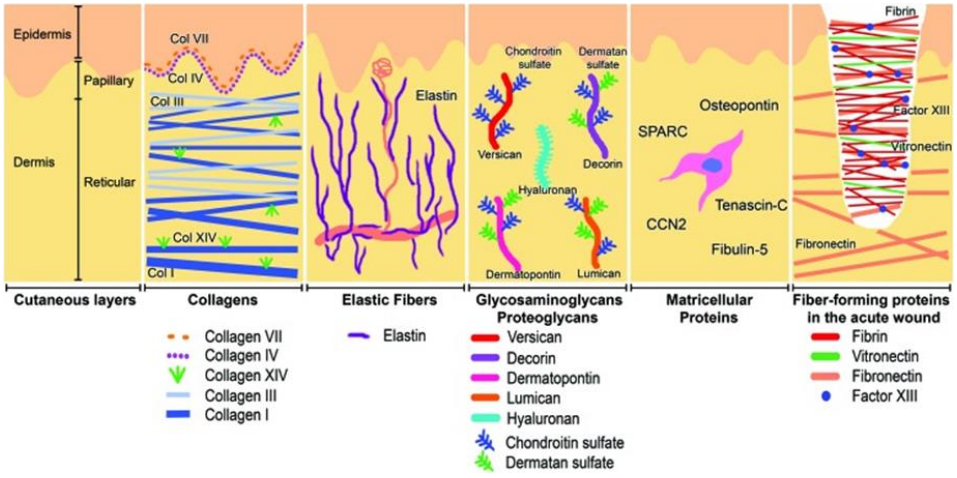

Figure 4 Depiction of major components of the ECM in normal skin. Structural ECM components include collagens and fibers; collagens impacting mechanical structure and fibers impacting elasticity. Various matricellular proteins are involved in cellular signaling. Note. Reprinted from "Extracellular Matrix and Dermal Fibroblast Function in the Healing Wound" by Tracy et al., 2016, Advances in Wound Care, Vol 5 number 3, p.122. Article published under an open access Creative Common CC By license.

1.4 Inflammation, Cancer, and Photoaging

Inflammation is a natural bodily response in which host defense mechanisms are activated in response to stressors. Stressors such as microbial infection, or signals such as tissue damage initiate inflammation to repair damage and regenerate cells (Rakoff-Nahoum, 2006). Acute inflammation in response to stressors is perfectly normal, but when our body is in a chronic state of inflammation there is a greater risk for deterioration and permanent damage. Prolonged inflammation is linked to aging and the predisposition to cancer development due to the formation of genomic lesions, leading to tumor initiation. If these lesions in our DNA are not detected during the closely regulated cell cycle and repaired by one of the many nucleotide repair mechanisms, they can accumulate as unrepaired DNA and lead to mutations that ultimately result in cancer (Rakoff-Nahoum, 2006) (Clancy, 2008). The process of cellular inflammation can be

detected and measured via proinflammatory markers, such as cytokines, that are associated with increased inflammation (Lago et al., 2019). Proinflammatory cytokines are released in a cycle initiated by UV radiation. When the skin is exposed to sunlight or other sources of UV radiation, reactive oxygen species (ROS) are produced in excess and deplete the antioxidant supply in the skin, resulting in oxidative stress. Oxidative stress itself is damaging to our DNA (as will be explained further) and it also results in the increase of pro-inflammatory cytokines and initiation of inflammation (Ansary et al., 2021). Many cytokines are secreted in the skin by UV exposure and ROS increase, including interleukin-1α (IL-1α), interleukin-2 (IL-2), interleukin-6 (IL-6), tumor necrosis factor α (TNF-α), and others. When secreted by senescent, or aging fibroblasts, IL-1α, IL-1β, IL-6, and IL-8 are known as senescence-associated secretory phenotype factors (SASP). SASP factors are detrimental as they promote chronic inflammation and lead to photoaging of the skin by degrading the extracellular matrix (Ansary et al., 2021).

Cancer is a broad term used to describe the uncontrolled proliferation of cells abnormal to surrounding tissue. While the complete process of carcinogenesis is not fully understood, many factors that are known to increase the risk of cancer (carcinogens) have been identified (2022-Cancer-Facts-and-Figures, n.d.). Ultraviolet light is one of the most common carcinogens, causing the most prevalent form of cancer in America - skin cancer (2022-Cancer-Facts-and-Figures, n.d.). Skin cancer is induced by harmful inflammation and DNA damage, which can be caused by overexposure to UV rays (D'orazio et al., 2013).

In addition to the possible deadly effects such as cancer, premature photoaging of the skin is a common adverse effect of the oxidative stress perpetuated by sUV exposure.

Photoaging is classified as a type of extrinsic aging, meaning it is caused by environmental factors, mainly sun exposure. Photoaging is commonly characterized by a decrease in the elasticity of skin, which manifests as excess wrinkling, as well as changes in pigmentation of the sun-exposed skin (Ryu et al., 2014).

1.5 sUV- induced DNA Damage

The sun's UV rays cause direct and indirect damage to our DNA and to our cells. The type of damage resulting from UV exposure depends on many variables other than wavelength of UV radiation, including the molecule that is absorbing the energy from the UV photons. Chromophores are molecules that directly absorb UV radiation and cause damage through a series of photo-induced reactions. Our DNA is included in this class of molecule, meaning it directly absorbs UV photons (Svobodova et al., 2006). As previously mentioned, UVC (specifically 260 nm) is the most dangerous wavelength of UV radiation because it is very easily absorbed by our DNA. Even though the UVC range of the Sun's radiation does not reach us, the remaining UVA and UVB wavelengths still cause damage as they are also absorbed by DNA (Juzeniene et al., 2011). Energy in the form of UV photons is absorbed by our DNA and causes rearrangements in the biochemical structure of DNA. The most frequent rearrangement occurs when UV radiation causes the cleavage of internal pyrimidine bonds. The lesions then cause nucleotides in DNA to experience abnormal bonding and rearrangements of the typical 3-dimensional structure of our DNA, resulting in photoproducts known as cyclobutane pyrimidine dimers (CPDs) and pyrimidine (6-4) pyrimidone photoproducts (6-4 photoproducts or 6-4PPs)

(D'orazio et al., 2013). It has been shown that CPDs and 6-4PPs are formed in both cultured keratinocytes and human skin when exposed to UVA and UVB light (Mouret et al., 2006).

Differences lie in the mechanisms with which CPDs are produced by UVA and UVB light. UVA exposure causes CPDs through a photosensitization reaction in which energy is transferred to the DNA instead of being directly absorbed (Mouret et al., 2006). UVB, however, causes mostly direct DNA damage and formation of CPDs. UVB has a greater ability to be directly absorbed by DNA, leading to lesions such as CPDs which occur preferentially by UVB over UVA exposure (Pfeifer, 2020).

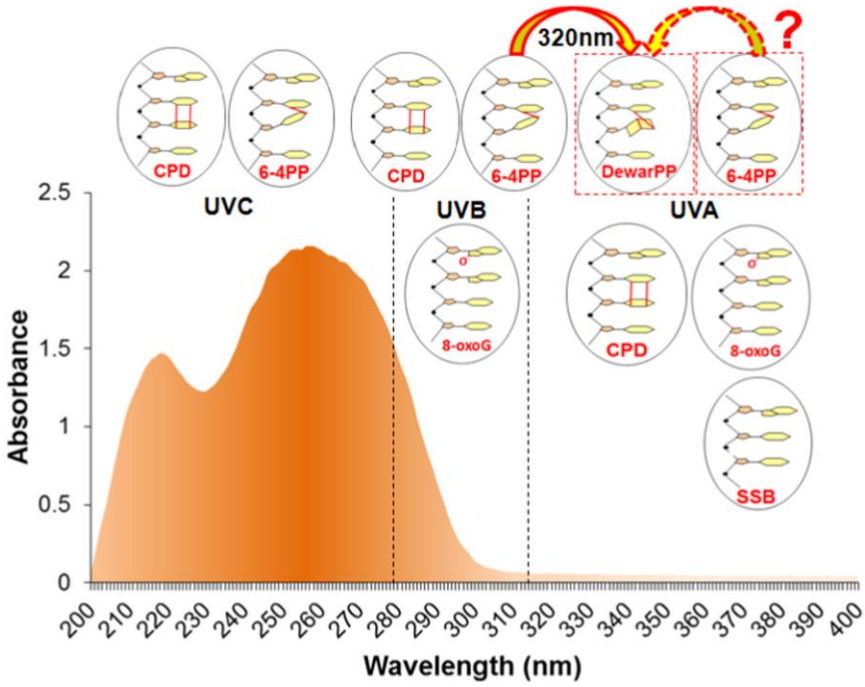

Figure 5 DNA absorption spectrum of UV light by wavelength and main forms of DNA damage arising from various wavelengths of UV radiation. "Sunlight damage to cellular DNA: Focus on oxidatively generated lesions" by Schuch et al., January 2017. Free Radical Biology and Medicine. http://dx.doi.org/10.1016/j.freeradbiomed.2017.01.029. Attribution-NonCommercial-NoDerivatives 4.0 International (CC BY-NC-ND 4.0)

The molecules that play a role in the indirect production of UV induced cellular damage are known as photosensitizers. Photosensitizers are molecules that absorb UV radiation and participate in certain photodynamic reactions. In Type I photodynamic reactions, an electron is abstracted from the photosensitizer molecule, forming a charged radical, or free radical. In Type II reactions, energy is transferred from the photosensitizer to molecular oxygen, forming oxygen in the first excited state, also known as reactive oxygen and nitrogen species (ROS and RNS) (Svobodova et al., 2006), (Cadet et al., 2015). Figure 6 below is a scheme of these photosensitization reactions. The chemical compounds formed by Types I and II photodynamic reactions interact with DNA to produce oxidative damage. Single stranded breaks, DNA crosslinks, and mispairing of DNA bases are common resultants of the increased ROS and RNS but are not the most frequent type of DNA lesions induced by sUV, as they are produced in lower quantities compared to CPDs (Cadet et al., 2012). Like the damage observed in direct UV absorption, CPDs can be formed via photosensitization. The mechanism suggested involves the transfer of energy from an excited chromophore to the DNA, specifically to thymine (Douki et al., 2003). In addition to these detrimental forms of cellular damage, the increase in ROS due to type II reactions overwhelm the body's antioxidant (AOx) defense systems and throw off the equilibrium of pro-oxidant and AOx chemicals, causing oxidative stress (Svobodova et al., 2006). Antioxidant stores are depleted in response to the reactive oxidative molecules formed after UV exposure.

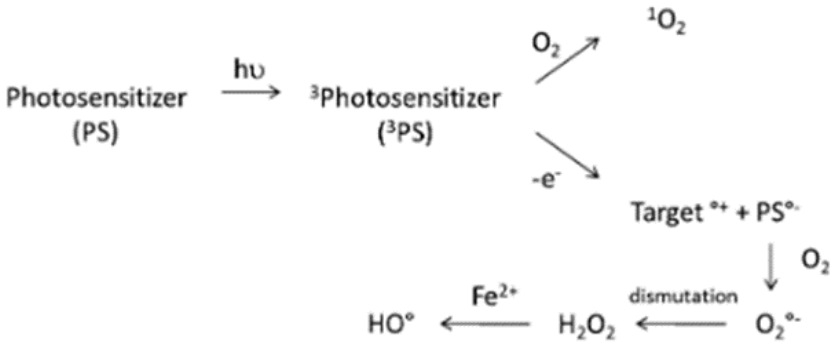

Figure 6 Type I and II photosensitization reactions forming reactive oxygen species. Note. Reprinted from "Oxidatively Generated Damage to Cellular DNA by UVB and UVA Radiation", by Cadet et al., 2015, Photochemistry and Photobiology, 91, p. 142. Copyright License Number 5537340053558

1.6 DNA Damage Repair

As previously mentioned, CPDs are the principal source of UV "signature" DNA mutation. This is because it is the major form of DNA damage formed from UV exposure. CPDs and 6-4PPs DNA lesions are removed by the Nucleotide excision repair (NER) mechanism with different efficiency, meaning CPDs are repaired slower than 6-4PPs due to the dramatic DNA-distorting nature caused by the presence of the 6-4PPs (Lee et al., 2020). This causes CPDs to persist in DNA up to 48 hours after UV exposure (Mouret et al., 2006) When unrepaired, CPDs interfere with the activity of DNA polymerase which may lead to the formation and accumulation of what are known as UV "signature" mutations, which are often observed in skin cancer lesions (D'orazio et al., 2013), (Walmacq et al., 2012), (Lee et al., 2020). As mentioned, CPDs are removed via NER, a process that is highly conserved in eukaryotes, involving many steps and proteins.

There are two main methods of DNA damage recognition that initiate NER in eukaryote; one being transcription coupled repair (TCR), the other being global genome repair (GGR) (Figure 7). Detection by TCR involves the recruitment of Cockayne Syndrome protein B (CSB), an ATP-dependent chromatin remodeling protein, and Cockayne Syndrome protein A (CSA) to the specific piece of damaged DNA. In cases where the transcribed strand is damaged, RNA polymerase II elongation is stalled during transcription to activate the TCR process (Lans et al., 2010). RNA polymerase is stalled to allow time for specific transcription-coupled proteins to recognize the DNA lesions. Once recognized, the DNA is stabilized, and the UV photoproducts are cleaved by endonucleases (Pfeifer, 2020).

When DNA damage is present in non-transcribed strands or regions of DNA, GGR scans the entire genome for distortion in the helix (Figure 7). Detection by GGR involves two protein complexes; UV-damaged DNA-binding protein complex (UV-DDB) and a complex containing Xeroderma Pigmentosum group C protein (XPC), human homolog of RAD23 (hHR23), and Centrin-2. XPC is a main detector of DNA damage, as it is able to detect the drastic changes in the DNA, such as those caused by 6-4PPs. Dimeric photoproducts that are less pronounced (CPDs) are recognized by the UV-DDB complex, which inserts into the dimer to directly interact and recruit XPC and other proteins and ubiquitin ligases to repair the DNA damage (Gsell et al., 2020).

After DNA damage recognition by either TCR or GGR, the NER pathway continues with first opening and stabilizing the DNA at the damage site (Pfeifer, 2020). Transcription factor IIH (TFIIH) complex, containing Xeroderma Pigmentosum group A and B (XPB and XPD) helicase

subunits, is recruited to the damage site. The helicase subunits unwind DNA at the site of damage, allowing Xeroderma Pigmentosum group A (XPA) and Replication Protein A (RPA) to bind, and stabilize the DNA. These factors also play a role in recruiting and properly orienting the structure-specific endonucleases. Xeroderma Pigmentosum group F -Excision Repair Cross-Complementing protein 1 (XPF/ERCC1) is recruited by XPA and makes the 5' cut while Xeroderma Pigmentosum group G (XPG) makes the 3' cut to fully surround the lesion. These two incisions allow the damaged DNA region to be removed in an oligonucleotide fragment, and the resulting gap is filled in by DNA repair synthesis (Gsell et. Al., 2020).

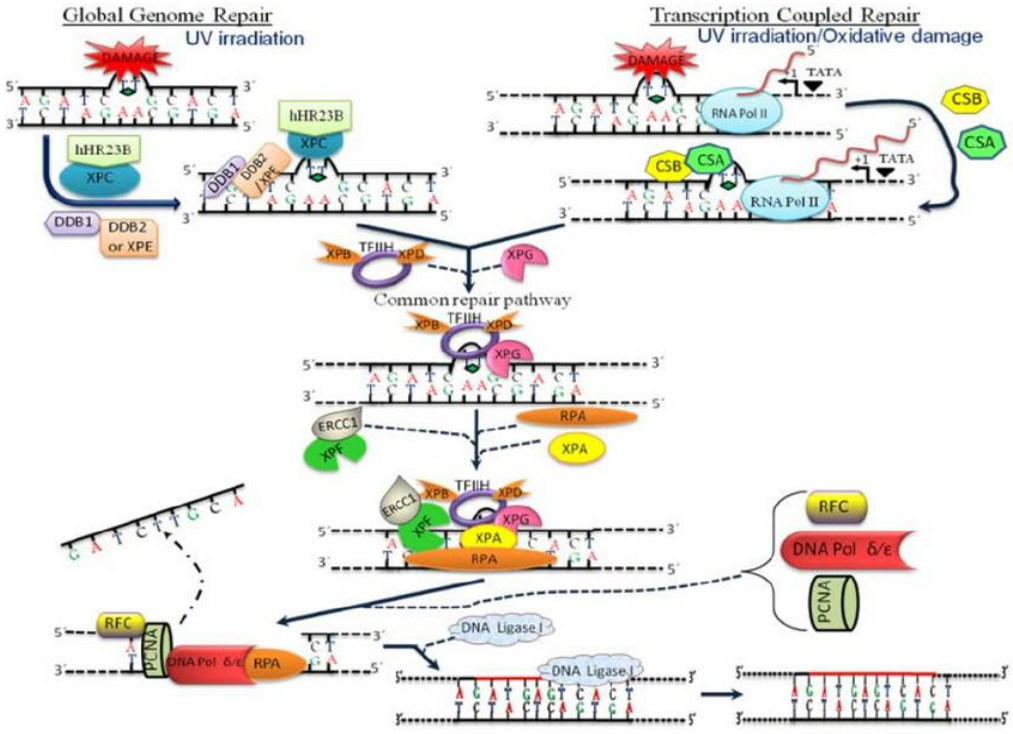

Figure 7 GGR and TCR recognition of DNA damage and the common NER pathway for removal of damage. "Head and Neck Squamous Cell Carcinoma: Prognosis using molecular approach" by Mazumder et al., September 2013. Central European Journal of Biology. 9. 10.2478/s11535-014-0292-3. Creative Commons Attribution-NonCommercial-NoDerivatives 3.0 License.

1.7 cNOS: A Target for Preventing UV Induced Damage

Common and effective prevention of these adverse effects of sun exposure include limiting overall exposure and utilizing physical and chemical sun block (i.e., SPF containing sunscreen and UV filtering clothing), but these may not be the only preventative treatments available. To discover new preventive treatments for UV-induced damage, new targets must be identified and researched. One possible target is an enzyme known as nitric oxide synthase (NOS), which is the primary source of nitric oxide (NO·) in most mammals (Li et al., 2014). NO· is a small gaseous signaling molecule found in many body systems and organs. This molecule plays a wide variety of roles throughout the body, and the effects can be different based on the specific location, organ, or cell in question. For example, in the central nervous system, NO· has been shown to play a role in synaptic plasticity and memory; in the cardiovascular system, NO· dilates blood vessels (Förstermann & Sessa, 2011).

There are three isoforms of the NOS enzyme - neuronal NOS (nNOS or NOS1), inducible NOS (iNOS or NOS2), and endothelial NOS (eNOS or NOS3), which are all located on different genes. nNOS and eNOS are constitutively expressed, and together known as cNOS (Costa et al., 2016), (Chen et al., 2008). NOS produces NO· through a series of redox reactions involving O_2 and the amino acid L-arginine (Chen et al., 2008). For NO· production, this enzyme forms a homodimer with an N-terminal oxygenase domain a C-terminal reductase domain. The oxygenase domain holds the heme active site and binding sites for cofactors such as tetrahydrobiopterin (BH4), molecular oxygen, and L-arginine substrate while the reductase domain holds the binding sites for the redox cofactors flavin mononucleotide (FMN), flavin

adenine dinucleotide (FAD), and nicotinamide adenine dinucleotide phosphate (NADPH), as shown in figure 8 (Li et al., 2014), (Groves & Wang, 2000), (Förstermann & Sessa, 2011). Figure 8 depicts these two domains of NOS and the reactions that take place within them. In the reductase domain of NOS, electrons from NADPH are transferred first to FAD and FMN, which then transfer electrons to the haem group in the oxygenase domain. Next, electrons at the haem site reduce and activate oxygen and oxidize L-arginine to L-citrulline and NO (Förstermann & Sessa, 2011).

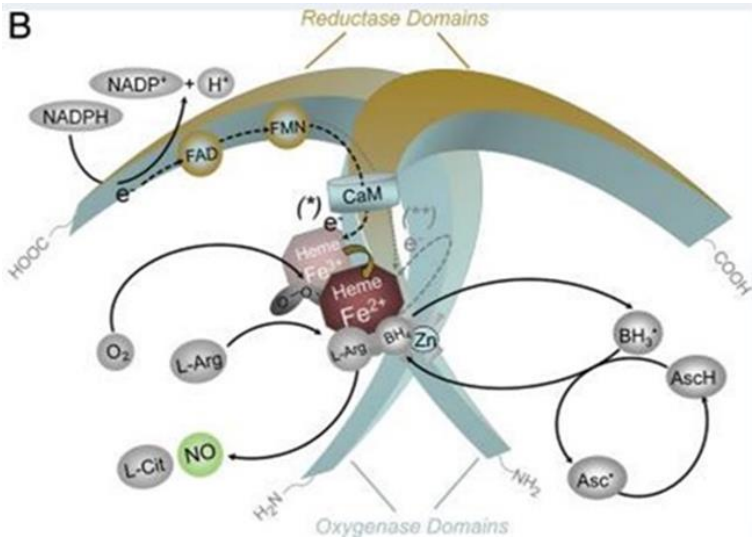

Figure 8 NOS homodimer containing N-terminal oxygenase domain with its respective cofactor binding sites and reductase domain with its respective binding sites. Redox reactions occur in the reductase and BH4 oxidation takes place in the oxygenase domains of nitric oxide synthase. Note. Modified from "Nitric oxide synthases: regulation and function", by Förstermann, U. and W.C. Sessa, 2011, European Heart Journal, 33(7): p. 831. Copyright License Number 5537310465904

Under certain conditions, the series of reactions involved in the synthesis of NO· are not coupled (known as "uncoupled cNOS") and instead of forming NO·, superoxide (O_2·−) is formed. Since NO· is abundant inside a cell, the O_2·− formed reacts with NO· forming the strong oxidant peroxynitrite ($ONOO^-$) (Alkaitis, Crabtree 2012). Uncoupling is a general term that describes the impairment of electron transfer between domains of the NOS homodimer. The electron transfer is necessary for the activation of O_2, which is crucial for the oxidation of L-arginine and the synthesis of NO·. Within the oxygenase domain, the cofactor BH4 is a key player in this electron transfer process, as well as for the stabilization of NOS homodimer, and the promotion of the catalytic activity of the NOS enzymes. This being said, any interference with BH4 bioavailability will have an effect on the electron transfer capacity of NOS. Factors that inhibit BH4 activity or decrease BH4 availability will cause NOS to produce O_2·− instead of NO·. As shown in figure 9, some factors that contribute to NOS uncoupling include decreased levels of L-Arginine, cellular oxidative imbalance [i.e. high levels of oxidized glutathione (GSSG) relative to reduced glutathione (GSH)], and the presence of NOS inhibitors (L-N-monomethylarginine L-NMMA) and asymmetric dimethylarginine (ADMA) (Alkaitis, Crabtree 2021).

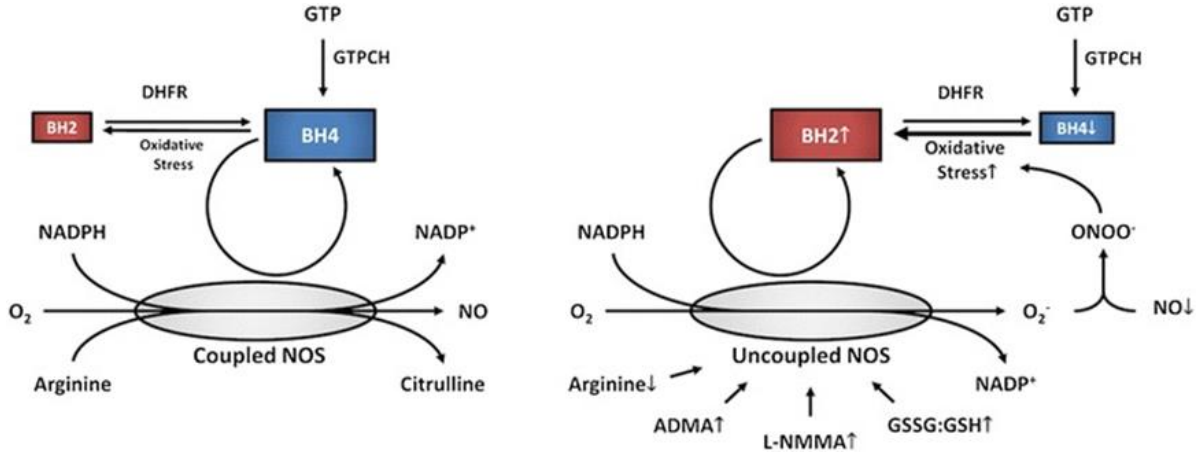

Figure 9 Proper coupled reaction leading to nitric oxide production versus the uncoupled reaction leading to peroxynitrate production. Note. Reprinted from "Recoupling the Cardiac Nitric Oxide Synthases: Tetrahydrobiopterin Synthesis and Recycling", by Alkaitis, M.S., Crabtree, M.J.. 2012, Curr Heart Fail Rep, Vol. 9, Issue 3, p. 203. Article published under an open access Creative Common Attribution License

As the name suggests, eNOS is responsible for the production of NO· in the endothelium, which is largely responsible for vascular tone, which refers to the muscle tone and contractility of blood vessels (Deanfield et al., 2007). nNOS is abundant in neurons and produces the NO· stores responsible for the function of neurons, which is necessary for the stimulation of muscles (Costa et al., 2016). In addition to the locations indicated by their names, all three isoforms are found throughout various cells in the body, including the cells in the skin. Figure 10 shows the locations of the three NOS isoforms within the skin. Keratinocytes, located in the epidermis, contain nNOS, eNOS, and iNOS, while fibroblasts, located in the dermis, contain eNOS and iNOS, shown in figure 10 (Frank et al., 2002), (Nilforoushzadeh et al., 2021). The constitutively produced NOS have increased activation immediately after UV exposure, but iNOS has an increased expression and activation in the late phase after UV exposure (around 6 hours post UV) (Hazell et al., 2022), (Kuhn et al., 1998), (Liu & Wu, 2010). The study conducted by Liu

and Wu in 2010 showed iNOS to be elevated at 6 hours and increased with time until 24 hours post-UV. Because iNOS is upregulated for a longer period than cNOS, iNOS is responsible for a bulk of the NO· found in the skin after UV exposure. The 2010 study also showed that the relative amount of NO· produced in immortalized human keratinocyte (HaCaT cells) peaked at 18 hours (Liu & Wu, 2010).

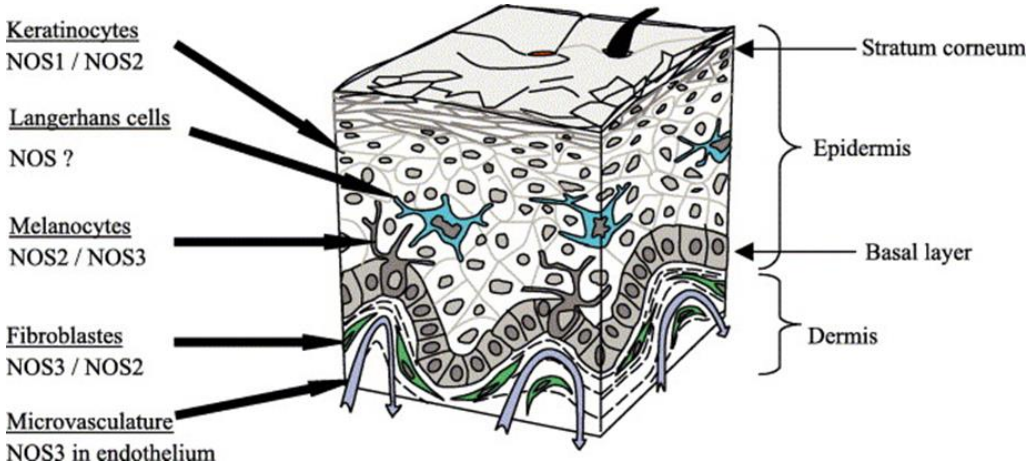

Figure 10 Subsection of the skin including epidermal and dermal cells as well as the NOS isoforms located within these skin cells. Note. Modified from "Nitric oxide function in the skin", by M.-M. Cals-Grierson and A.D. Ormerod, 2004 , Nitric Oxide, 10, p. 181. Copyright License Number 5537350133339

1.8 Role of cNOS in UVB Irradiated Keratinocytes

A study was previously conducted by Dr. Tong and Dr. Wu at Ohio University to further our understanding of the impacts of RNS in immortalized human keratinocyte (HaCaT cells). In this study, cNOS activity was stopped with the treatment of the selective inhibitor L-NAME (L-N^G-Nitro arginine methyl ester). The cells were then exposed to UVB radiation and analyzed via ELISA, western blot, and other assays to determine the activity of the NF- κB transcription

factor. NF- κB is a class of inducible transcription factors and is involved in the body's immune and inflammatory processes, as well as in cancer development and progression. (Xia et al., 2018). This study found UVB induced synthesis of NO· and $O_2 \cdot -$ caused the stimulation of the NF- κB pathway in keratinocytes, which ultimately could lead to carcinogenesis by its pro-survival activity (Tong & Wu, 2014).

The mechanism proposed by these authors involved the phosphorylation of the α-subunit of eukaryotic initiation factor 2 (eIF2α), which causes the inhibition of the global protein synthesis by inhibiting the initiation step of translation. After UVB exposure, cNOS activation and further uncoupling increased the levels of phosphorylated eIF2α (p-eIF2α) mediated by the eIF2α kinases GCN2 (general control nonderepressible protein kinase 2) and PERK (PRKR-like endoplasmic reticulum kinase). GCN2 is activated by amino acid starvation, so the depletion of L-Arginine that occurs due to initial NO· synthesis may elevate levels of p-eIF2α, in addition to inducing cNOS uncoupling (Jiang & Wek, 2004), (Tong & Wu, 2014). The mechanism of PERK activation after UVB exposure is unknown.

Due to the protein synthesis inhibition induced by p-eIF2α, the levels of IκB (inhibitor of NF- κB) decrease, allowing the activation of NF- κB. This effect was avoided when cNOS was chemically inhibited, suggesting that inhibition of cNOS is necessary for avoiding the phosphorylation of eIF2α and protecting the keratinocytes from the IκB loss and NF- κB activation after UVB exposure. This study observed that both eNOS and nNOS are involved in the regulation of this response. The activation of NF- κB protects keratinocytes from apoptosis

induced after UVB radiation. This anti-apoptotic effect was observed to be neutralized by the elevated levels of ONOO- induced by cNOS uncoupling post-UVB (Tong & Wu, 2014).

1.9 Role of cNOS in UVB induced DNA damage and carcinogenesis.

The role of cNOS in the induction of CPDs and skin cancer lesions was studied previously in our lab. Since *in vitro* studies showed that $ONOO^-$ and $NO^{\cdot}$ donors induce the formation of CPDs, the role of cNOS was then analyzed *in vivo*. In these preliminary studies, the protective role of Nω-Nitro-L-arginine methyl ester (L-NAME, a cNOSs inhibitor) against UVB was evaluated. Mice were irradiated for 6 (group 1) and 28 weeks (group 2), 3 times per week, in the presence or absence of topical L-NAME. At week number 6, the results showed that the female mice treated with L-NAME contained fewer epidermal cells positive for CPDs compared to the control mice. At week 28, the mice treated with L-NAME showed fewer skin lesions than the controls, and their tumors were also smaller in surface area. However, no differences were observed either at 6 or 28 weeks in male mice. These results strongly suggest that in the female group, the inhibition of cNOS was an important factor involved in the development of skin damage and carcinogenesis, which should be further explored. (Bahamondes, 2020)

Unexpectedly, unpublished results in this lab using cNOS KO mice, show that compared to the controls, the KO mice develop more skin lesions when exposed to sUV (Zhou, 2022). Since this data does not match the results obtained previously with the cNOS inhibitor, further exploration is required. Due to the known impacts of ROS and NOS produced after UV exposure and the specific study done with cNOS inhibition in human keratinocytes and *in vivo*. I

conducted a study to determine the effects of the genetic inactivation of cNOS on fibroblast cells after sUV exposure. This is where the current gap in our knowledge exists, so it is important to explore the role of cNOS in fibroblasts' cellular response to UV exposure. For my experiments, we utilized fibroblasts extracted from these mice with genetic alterations to the cNOS enzymes (cNOS KO), instead of treating the WT cells with a selective cNOS inhibitor.

2. Experimental Designs and Methods

2.1 SKH1 Mice Model

The SKH1 model corresponds to a mice strain characterized for developing alopecia early after their development. Due to being hairless, these mice are widely used in dermatological research, since they can be immediately manipulated without the need for shaving (Benavides et al, 2009). The cNOS KO SKH1 mice were developed using CRISPR/Cas9 technology by the company TransViragen Inc. The NOS1 (nNOS) and NOS3 (eNOS) genes are located approximately 46 centimorgans (cM), a unit of measure for the frequency of genetic recombination) apart on mouse chromosome 5. The strategy used by TransViragen Inc. for creating the nNOS KO was to remove the exon 10 using guide-RNAs (gRNAs) and primers directed to the intron 9 and 10 of the nNOS gene. For the development of eNOS KO, the strategy consisted of using gRNAs and primers directed to the introns 3 and 4 of the eNOS gene for removing exon 4. The deletion of the mentioned introns will introduce a translational frameshift with downstream premature stop codons. This change should trigger nonsense-mediated mRNA

decay, meaning that nNOS and eNOS proteins are not going to be expressed when the mutation is present.

2.2 Cell Extraction

As previously mentioned, this study was conducted using primary fibroblasts isolated from SKH1 hairless mice. The mice used were bred to express various combinations of cNOS genes, and typically died due to complications of these gene deletions. These health issues related to the cNOS knockout (KO) made them unfit for long-term experiments. After the mice died naturally or were euthanized due to IACUC requirements, skin samples were extracted from the mice following protocol adapted from “Murine Dermal Fibroblast Isolation " by Walmsey et al. In order to extract the skin, the mice were first sterilized in 70% ethanol alcohol for at least 15 minutes. The mice were placed in appropriate-sized beakers to compensate for the size of the mouse, then covered in the ethanol solution. After this initial sanitization of the mice, UV-sterilized processing equipment consisting of tweezers and small scissors were used to dissect the dorsal skin from the mice, avoiding the limbs and any large fat deposits typically located in the abdominal and lateral abdominal regions of the mice. The skin samples were cut to roughly 1.5 cm^2 pieces. As shown in figure 11, the skin samples were first rinsed with a solution of 1X PBS and Gentamicin (50 ng/mL, Gibco, #15750-060) to sterilize the skin. Next, the skin was treated with a cold 0.5 % dispase solution (5 U/mL dispase in Hanks' Balanced Salt Solution, #07913, Stemcell™) in DMEM medium (Corning™, Cell gro™, 10-013-CV) and incubated at 37°C for 45 minutes. This solution allowed for the separation of the epidermis and dermis. After rinsing with PBS, the skin layers were separated, and the epidermis was discarded. The dermis

was incubated in a 15 mL tube with 10 mL of collagenase type IV (1 mg/mL, Gibco, #17104-019) in DMEM to allow the isolation of individual cells. After centrifuging and collection of the pellet, the cells were seeded on gamma-irradiated treated cell culture plates and grown in DMEM medium (Corning™, Cell gro™, 10-013-CV) supplemented with 10 % v/v FBS, and 1 % v/v penicillin/streptomycin, at 37°C with 5 % CO_2 (figure 11). Primocyn™ (100 µg/mL, Invivogen, #ant-pm-05) and Fungin™ (10 µg/mL, Invivogen, #ant-fn-1) were added to the cell culture medium and maintained during 5 days to prevent microbial and fungal contamination.

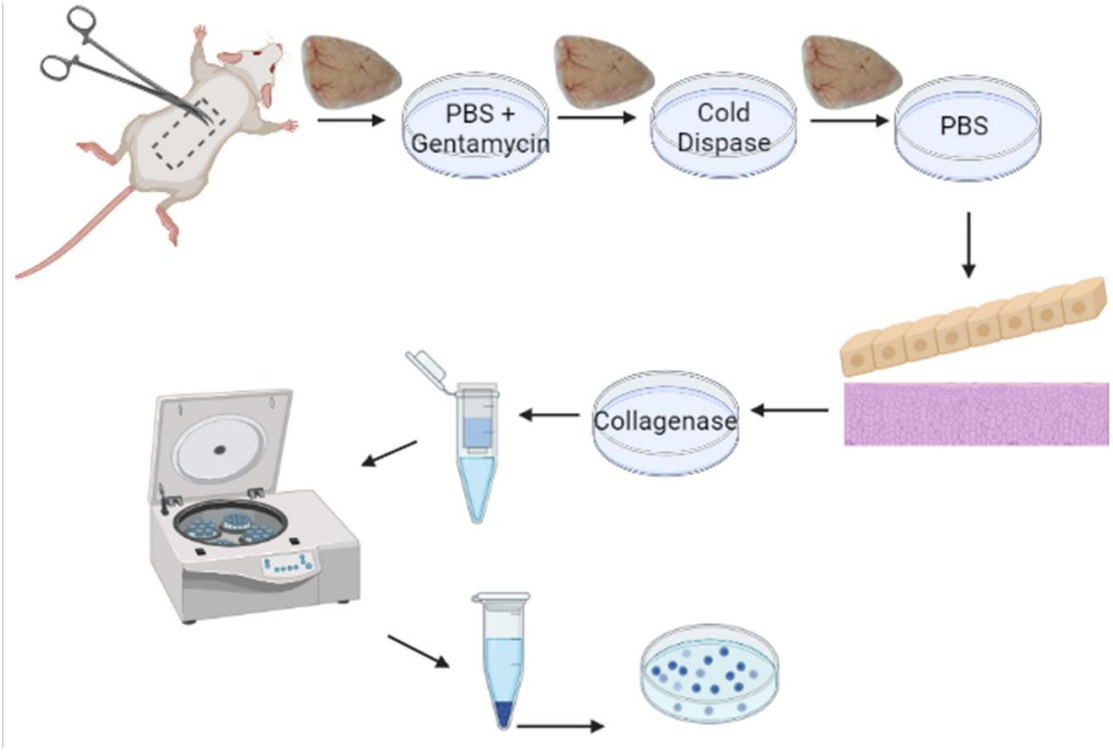

Figure 11 Visualization of skin extraction and fibroblast isolation procedure. Procedure is adapted from “Murine Dermal Fibroblast Isolation " by Walmsey et al. The skin is first dissected from the back of the mice avoiding large fat deposits and mammary glands. The tissue is then disinfected, the layers are separated, and the dermis is isolated followed by the separation of individual cells. After filtering and centrifuging, the fibroblasts are seeded onto the treated culture medium plates and grown in supplemented DMEM medium. Image created with Biorender.com.

2.3 sUV Irradiation

To prepare for sUV irradiation of the fibroblast cells, the fibroblasts were seeded onto 60mm gamma-irradiated treated cell culture plates the day before irradiation. First, the sUV lamp (UVA-340 lamp, Q-lab,Co.) was turned on at least 10 minutes prior to cell irradiation to warm it up and stabilize its emission intensity (Figure 12). Samples were irradiated with 200 mJ/cm^2 of UVB with a dose rate of 0.16 ± 0.01 mW/cm^2 per second. The UVB intensity was measured using the UVX digital radiometer (UVP, Inc) attached to a UVX-31 UVB sensor (UVP, Inc). The time for irradiation was then calculated using a previously calculated correction factor for this lamp, according to Bahamondes Lorca et al., 2022, which utilized the measured intensity and desired dose of UVB.

The plates were between 70~90% confluent at the time of irradiation to maximize results. To prepare the cells for irradiation, the medium was removed and the plates were rinsed with 1X PBS solution. After removing this PBS, 2mL of 1X PBS was added to the plates and remains during sUV exposure. For the control cells, the plate remained in the fume hood with air circulation on and the lid off for the calculated amount of time. For the sUV exposed cells, the plates were left under the sUV lamp without the lid for the calculated time. The sUV lamp was turned off at the end of the exposure period and all plates were taken back to the fume hood. The PBS was removed from all plates and 1.75mL of medium was then added to each plate. The plates were then placed back in the incubator for the allotted amount of time, which is determined by the tests being done after irradiation. For protein extraction from irradiated cells, the plates were incubated for 1 hour and 3 hours after sUV irradiation. At the end of the

incubation period post-sUV irradiation, the medium was collected and stored at -80° C, and the cells were rinsed with 1X PBS in preparation for protein extraction. For DNA extraction after sUV irradiation, extraction took place immediately after sUV irradiation and after 20 minutes of incubation.

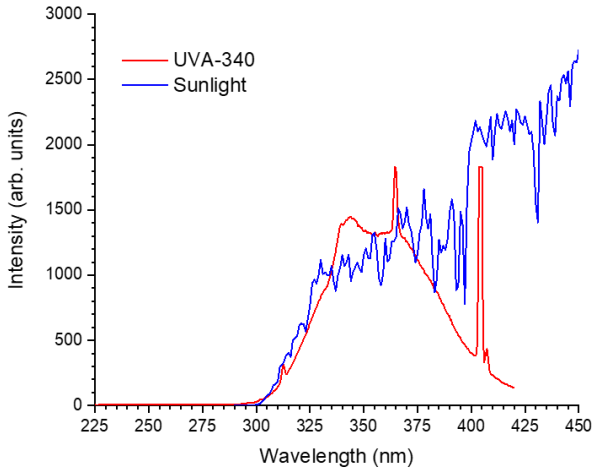

Figure 12 Spectrum of UVA-340 lamp used in comparison to the spectrum of Sunlight. Note. Modified from"Characterization of UVB and UVA-340 Lamps and Determination of Their Effects on ER Stress and DNA Damage", by Bahamondes Lorca, V.A., McCulloch, M.K., Ávalos-Ovando, Ó., Govorov, A.O., Rahman, F. and Wu, S. (2022). Photochem Photobiol, 98: 1140-1148. https://doi.org/10.1111/php.13585 . Copyright License Number 5537360550525

2.4 DNA Extraction

DNA extraction was performed using the commercially available kit from Qiagen, DNeasy Blood and Tissue Kit (#69504). The manufacturer's protocol for this kit was used, starting with cultured cells. Briefly, cultured fibroblasts were first centrifuged down into a pellet that was then resuspended in 200 µL PBS, plus 20 µL proteinase K. 200 µL of Buffer AL

(included in kit) was added and the samples were mixed by vortexing. The samples were then heated at 56 ° C for 10 minutes, followed by the addition of 200 µL 100% molecular grade ethanol. The samples were then transferred from the microcentrifuge tube into the DNeasy Mini spin column placed in a 2 mL collection tube, and centrifuged at 8000 rpm for 1 min. The spin column was then washed with Buffer AW1 and Buffer AW2 before being transferred to a new microcentrifuge tube. Finally, the DNA is eluted by adding 100 µL Buffer AE to the spin column, incubated for 1 min at room temperature, and centrifuged for 1 minute at 8000 rpm. This final step to elute the DNA was repeated in order to increase the DNA yield.

2.5 PCR for Genotype Characterization

To verify the genotype and sex of the fibroblasts, multiple PCRs (polymerase chain reaction) were performed using DNA extracted from the tails of the mice, as well as from the fibroblasts. To start, DNA extraction solutions 1 (25mM NaOH, 2mM EDTA) and 2 (40mM Tris-HCl) were freshly prepared. 100 µL of solution 1 was first added to the cell pellet or the tail clipping, and heated at 95 °C for 1 hour. 100 µL of solution 2 was then added and the samples were mixed by vortexing. The samples were then centrifuged and the supernatant containing the DNA was collected and used for PCR.

The DNA samples were quantified using a spectrophotometer. These quantifications were then used to calculate the volume of DNA needed to get to our desired concentration of DNA. Typically, 15 µg/µL of DNA was used with GoTaq® Green Master Mix, 1X final concentration (M712, Promega), RNase/DNase free water, and primers (table 1). The

temperature cycles for PCRs determining genotype consisted of: 95 ℃ for 2 minutes; 14 cycles of 95 ℃ for 30 seconds, 72 ℃ for 30 seconds (reducing 1 ℃ per cycle), and 72 ℃ for 30 seconds; 24 cycles of 95 ℃ for 30 seconds, 58 ℃ for 30 seconds, 72 ℃ for 30 seconds; ending with 72 ℃ for 5 minutes. The samples were then analyzed by running them on 4% agarose/boric acid gel with 1X TBE buffer. The PCR protocol for sex determination was as follows: 94 ℃ for 2 minutes; 35 cycles of 94 ℃ for 30 seconds, 57 ℃ for 30 seconds, 72 ℃ for 30 seconds; ending with 72 ℃ for 5 minutes. The samples were then analyzed by running them on 2% agarose/boric acid gel with 1X TBE buffer.

Table 1. Primers used for characterization of each mouse and fibroblast primary cell line

nNOS KO Fw: 5'- ACTCTCAGAGTGAAAGACACGCTAGG -3' **nNOS KO** Rv: 5'- ACTTGCCGTTAGGACATTTGCTAA -3' Expected product from Nos1Del10 allele: 498 bp Expected product from WT allele: none	**nNOS WT** Fw: 5'- ACTCTCAGAGTGAAAGACACGCTAGG -3' **nNOS WT** Rv: 5'- CCAACAAGATCAGCACTGTTATTTGTG -3' Expected product from Nos1Del10 allele: none Expected product from WT allele: 512 bp
eNOS KO Fw: 5'- ACCTGATCCTGGCCTTTGTGTC -3' **eNOS KO** Rv: 5'- GGGAGAAGGTGATTTGTGACAGG -3' Expected product from Nos3Del4.1 allele: 473 bp Expected product from WT allele: 1186 bp	**eNOS WT** Fw: 5'- ACCTGATCCTGGCCTTTGTGTC -3' **eNOS WT** Rv: 5'- CAGGAGCTTCCTGGATCTGTTCA -3' Expected product from Nos3Del4.1 allele: none Expected product from WT allele: 541 bp
SXF: 5' - GATGATTTGAGTGGAAATGTGAGGTA – 3' **SXR**: 5' - CTTATGTTTATAGGCATGCACCATGTA – 3' Expected product in XY males: 280bp Expected product in XX females: approximately 480bp and 660 bp. (McFarlane et al., 2014) Primer from Sigma-Aldrich	**Zfy F**: 5' - GACTAGACATGTCTTAACATCTGTCC – 3' **Zfy R**: 5' - CCTATTGCATGGACTGCAGCTTATG – 3' Expected product in XY males: approximately 200bp Expected product in XX females: approximately none. (McFarlane et al., 2014) Primer from Sigma-Aldrich

2.6 ELISA

For CPDs identification, DNA extracted with the commercial Kit from Qiagen (DNeasy Blood and Tissue, #69504) was used. The formation of CPDs in the DNA samples was detected and quantified using OxiSelect™ UV-Induced DNA Damage ELISA Kit from Cell Biolabs Inc.

(STA-322). The manufacturer's protocol was followed for this assay. Following extraction with the DNeasy Blood and Tissue kit, DNA samples were converted to single-stranded DNA by heating at 95° C for 10 minutes, followed by chilling on ice for 10 minutes. DNA samples were then diluted to 0.8 µg/mL in 1X TE buffer pH 8.0, then added to the DNA High-Binding plate. DNA binding solution was added to the samples and the plate was incubated on an orbital shaker at room temperature overnight. DNA standards were also included and assayed with the DNA unknowns. After overnight incubation, the solutions were removed, the wells were washed with PBS, and the wells were blocked with the Assay Diluent. After incubating for 1 hour, this solution was removed and the Anti-CPD Antibody was added and incubated for 1 hour. The wells were then washed 5 times with Wash Buffer before the addition of Secondary Antibody-HRP Conjugate. After 1 hour of incubation, Stop Solution was added, and the absorbance was read at 450 nm.

The identification of the inflammatory markers IL1, IL6, and TNF-α in culture medium was performed using DuoSet™ ELISA kits from bio-techne R & D Systems (DY400, DY406, DY410). After sUV irradiation, medium was added and the cells were incubated for 1 and 3 hours. After the designated time, the medium was collected and used for inflammatory marker ELISA assays, following the manufacturer's protocol for each kit. Briefly, after reagent and plate preparation, the samples and standards were added to the plates, covered, and incubated for 2 hours at room temperature. After 3 aspirations/washings with Wash Buffer, Detection Antibody was added and allowed to incubate for 2 hours. Aspiration/washing was repeated after incubation with the Detection Antibody, followed by the addition of Streptavidin-HRP, incubation for 20

minutes, and aspiration/washing. Substrate Solution was then added, followed by Stop Solution and absorbance reading at 450 nm and 540 nm.

2.7 Protein Extraction

After sUV irradiation, medium removal, and PBS rinsing (and removal of PBS), 120 µL of protein extraction buffer was added to the cells. The protein extraction buffer used contained Radioimmunoprecipitation assay (RIPA) buffer (100 mM Tris-HCl, 2% v/v Triton X-100, 300 mM NaCl, 0.2% w/v SDS, 10 mM EDTA, and 1% w/v sodium deoxycholate) with 1X of the phosphatase and protease inhibitors, PhosSTOP (Roche, 4906845001) and Complete (Complete, Mini, EDTA-free Protease Inhibitor Cocktail, Roche, 11836170001), respectively. Immediately after the extraction buffer was added, the plate was scraped with a cell scraper for approximately 1 minute, being careful to scrape the entire surface of the plate. The contents were then collected into a microcentrifuge tube and kept on ice until all protein was collected for that experimental set. The samples were then centrifuged at 4° C and 12,000 rpm for 10 minutes, and the supernatant was collected and stored at -80° C. After protein extraction, quantification was performed using the DC protein assay (Bio-Rad Laboratories, Inc.) to determine the concentration of protein in the samples so that further analysis of the proteins could be done.

2.8 Western Blot

30 ug of proteins were separated by SDS-PAGE and transferred to a Nitrocellulose membrane (pore size 0.2 µm, Pall Laboratory, 66485). The membrane was blocked in 5 % w/v milk in Tris-buffered saline plus Tween 20 (TBST) for 1 hour and then incubated overnight with

the antibodies anti: iNOS (D6B6S, 1:1000, # 13120, Cell Signaling Technology®), NOS1 (R20, 1:500, # sc-648, Santa Cruz Biotechnology Inc.), β-actin (C4, 1:1000, # sc-47778, Santa Cruz Biotechnology Inc.), MMP2 (IM33, Ab-3, 1:1000, # 42-5D11, Millipore Sigma), and MMP1 (1:1000, # GTX100534, GeneTex Inc.) diluted in TBST. After washing, the membranes were incubated with the corresponding HRP-conjugated-secondary antibody (anti-mouse # 7076, 1:3000 and anti-rabbit # 7074, 1:2000; both from Cell Signaling Technology®) for 1 h at room temperature in 5 % w/v milk in TBST. The membranes were developed using the West Pico SuperSignal chemiluminescent substrate (Thermo Fisher Scientific, 34580) or the Western Sure PREMIUM chemiluminescent substrate (LI-COR Biosciences, 926-95000). Images were obtained from Odyssey® Fc Imaging System (LI-COR Biosciences) and quantified using the software Image Studio Lite (LI-COR Biosciences).

2.9 Statistical analysis

Each experiment was repeated at least three times. The scatter dot plot (figure 15) shows the mean (line) and S.D (error bar). The bar plot (figure 17) expresses the mean values ± S.D. The significance of the differences between mean values was assessed using Student's t-test. P-values smaller than 0.05 were considered significant.

3. Results

3.1 NOS Characterization

To study the role of solar UV induced activation of cNOS in skin cells, an *in vitro* model was established using fibroblasts isolated from cNOS KO mice. The aims of this thesis were to investigate the role of cNOS in DNA damage and repair, inflammation, and photoaging. In order to carry out the experiments necessary to investigate these aims, a large stock of fibroblasts encompassing many genotypes was needed. Table 2 lists all genotypes of primary fibroblasts collected, as well as the number of different cell lines, each collected from individual mice. To determine the genotype of the mice the fibroblasts were isolated from, PCRs were performed using DNA extracted from tail clippings. Below are the results after running the DNA samples on 4% agarose gel.

Table 2: Genotypes of collected fibroblasts and number of cell lines obtained from individual mice

Cell Line Genotypes		**Number of collected cell lines**
nNOS +/+ eNOS +/+	Wild type	6
nNOS -/- eNOS -/-	Double knock-out	2
nNOS +/+ eNOS -/-	nNOS WT eNOS KO	1
nNOS +/- eNOS -/-	nNOS heterozygote eNOS KO	2
nNOS -/- eNOS +/-	nNOS KO eNOS heterozygote	1
nNOS -/- eNOS +/+	nNOS KO eNOS WT	1

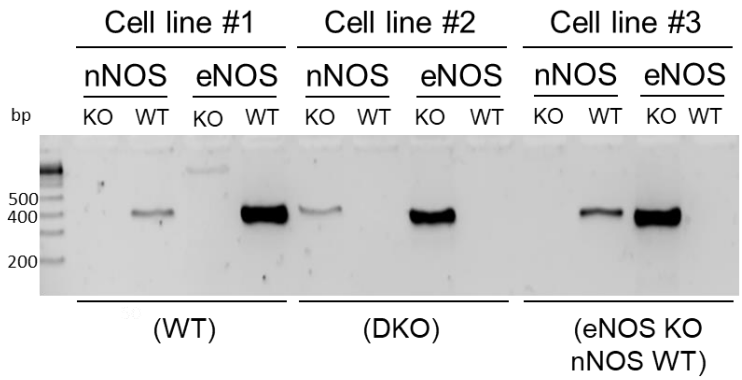

Figure 13 PCR representative image of genotyping of 3 different primary fibroblast cells, run on agarose gel 4%. In the figure, cell line 1 is nNOS WT and eNOS WT, cell line 2 is nNOS KO and eNOS KO (DKO), and cell line 3 is eNOS KO nNOS WT.

To identify which NOS enzymes were present in the fibroblasts, and determine if sUV irradiation affect these levels, Western blots were performed with protein extracted from sUV irradiated and control fibroblasts with WT, DKO, and eNOS KO/nNOS WT genotypes. All NOS isoforms were tested for (nNOS, iNOS, and eNOS), but only nNOS and iNOS gave consistent results. Below in figure 14 is one result of the three western blots performed for these proteins. Beta-actin protein levels were considered as the loading control to normalize protein levels. nNOS signal is detected in WT and eNOS KO/nNOS WT samples, and in control (no sUV) and sUV irradiated samples evenly. iNOS was detected in WT samples, and slightly in the eNOS KO/nNOS WT samples. There does not seem to be significant differences between the control and sUV irradiated samples for iNOS detection.

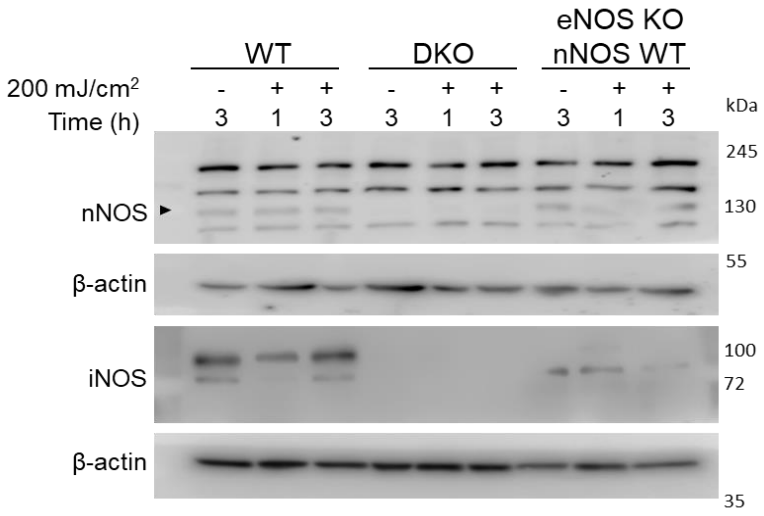

Figure 14 Western blot gel of various sUV and control showing protein expression of nNOS and iNOS in fibroblasts isolated from SKH1 mice. For nNOS, A band of 130 kDa is detected in WT and eNOS KO/nNOS WT cells, but not in the DKO cell line. No differences are observed between irradiated and no irradiated samples. The arrow shows the specific band for nNOS. iNOS is detected around 72 and 100 kDa. Bands for iNOS are not observed in the DKO cell line. N=2.

3.2 CPD Detection for DNA Damage Analysis

With the commercial ELISA kit from Cell Biolabs Inc, CPD levels were analyzed using DNA extracted from control and sUV irradiated WT, DKO, and eNOS KO/nNOS WT fibroblast. Below in figure 15 are the results from this experiment. In the WT samples, there was a significant increase in CPDs immediately after sUV irradiation. After incubating the WT cells for 20 minutes upon sUV irradiation in normal growth conditions, there was a significant decrease in CPDs. However, this pattern was not present in the DKO and eNOS KO/nNOS WT samples. These samples exhibited a significant increase in CPDs immediately after sUV

irradiation, followed by a further increase in CPD levels after the 20 minutes of incubation with the same standard growth conditions.

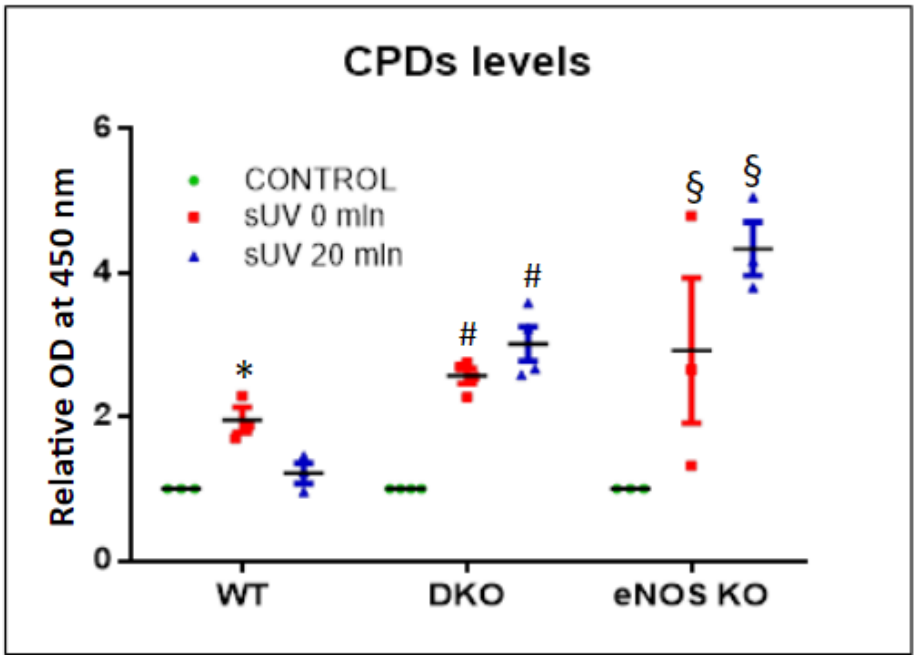

Figure 15 Scatter dot plot showing the quantified levels of CPDs detected with Cell Biolabs Inc. commercial ELISA kit. WT cells had an increase in CPDs immediately after sUV, which then decreased after 20 minutes incubation. The KO fibroblasts exhibited similar increase in CPDs immediately after sUV, but then a further increase after 20 minutes, not present in WT samples.* = statistical analysis against control WT. # = statistical analysis against control DKO. § = statistical analysis against control eNOS KO. N = 3.

3.3 MMP and IL Detection for Inflammatory and Aging Analysis

MMP1 and MMP2 proteins were analyzed in control and sUV irradiated samples extracted from control and sUV irradiated WT, DKO, and eNOS KO/nNOS WT fibroblasts. As shown in figure 16, the Western blot results from these experiments showed an increase in the

presence of cleaved-MMP1 (meaning the active form of the protein) after sUV irradiation. This pattern is present in WT, DKO, and eNOS KO/nNOS WT samples, showing increased MMP1 levels after irradiation. Pro-MMP2 (meaning the inactive form) and cleaved-MMP2 (active form) were detected in the WT samples. In the DKO samples, there were higher levels of pro-MMP2, in comparison with the eNOS KO/nNOS WT samples, which showed higher levels of cleaved-MMP2. There was no detected difference in MMP2 levels between the control and sUV irradiated samples.

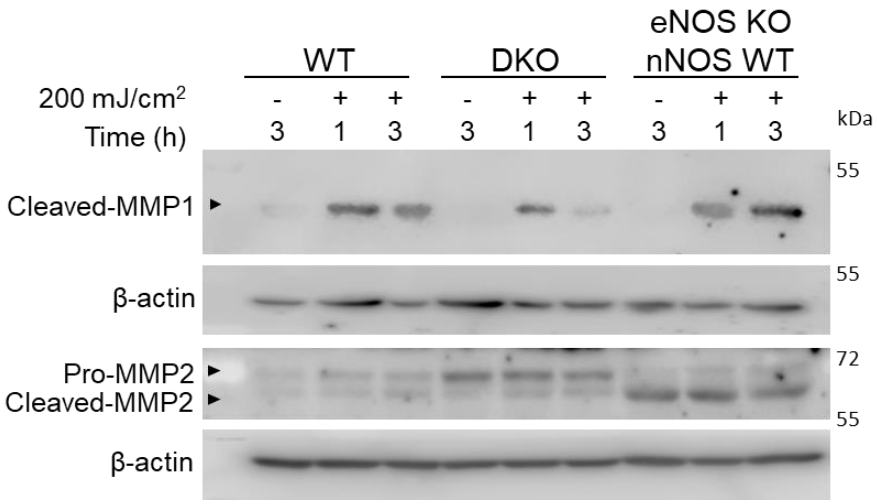

Figure 16 Western blot results showing protein expression of MMP1 and MMP2 in fibroblasts isolated from SKH1 mice at times 1 and 3 hours after sUV exposure. Cleaved MMP1 is detected at ~46 kDa while MMP2 is detected at ~72 (pro-MMP2) and ~63 (cleaved-MMP2) kDa. Protein levels of MMP1 increase after sUV irradiation but no significant differences are observed between the different cell lines. For MMP2, the WT cell expresses similar levels of pro- and cleaved-MMP2, while the DKO cell line shows higher levels of pro-MMP2. eNOS KO/nNOS WT cell line showed more levels of the cleaved MMP2. In the 3 cell lines, no significant differences are observed between irradiated and no irradiated samples. N=2

To evaluate the levels of IL1, IL6, and TNF-α cytokines after sUV irradiation, commercial ELISA kits from R&D Systems were used. Culture medium was collected from the WT, DKO, and eNOS KO/nNOS WT fibroblasts that were used for the various sUV Irradiation experiments. The levels of IL1 and TNF-α were below the detectable range, and these results are not shown. Below is the result of the ELISA for IL6. As shown, there are significantly higher levels of IL6 cytokine in the WT samples compared to eNOS KO/nNOS WT and DKO samples, with the DKO levels being the lowest. Unexpectedly, there are higher levels of IL6 in the control samples compared to the sUV irradiated samples.

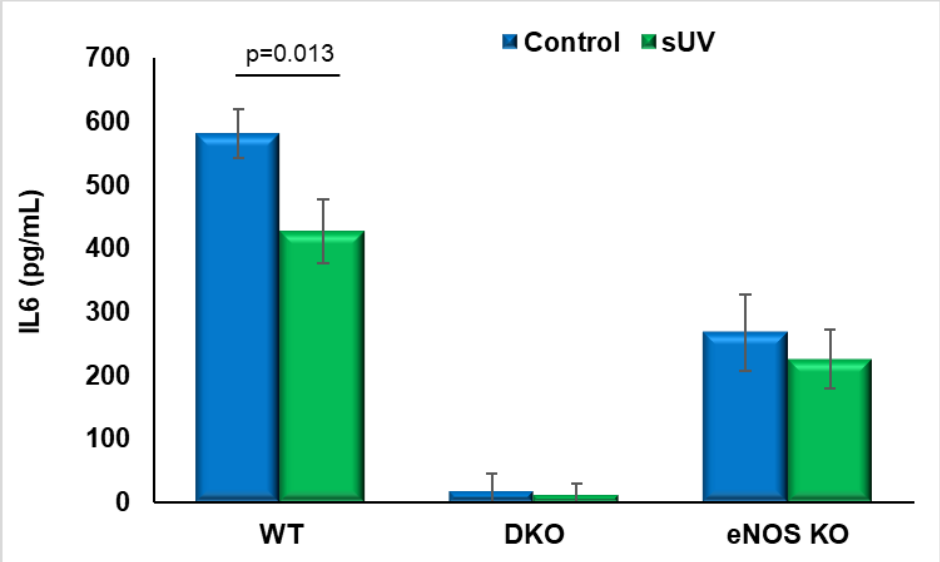

Figure 17 bar graph showing the IL6 levels in control and sUV irradiated samples from WT, DKO, and eNOS KO/nNOS WT culture medium. N = 3.

4. Discussion

To understand what the role of cNOS is in fibroblasts' cellular response to sUV exposure, we investigated the effects of knocking out the cNOS genes in fibroblasts. Specifically, cNOS's

role in fibroblast DNA damage levels, inflammatory response, and initiation of aging post sUV irradiation were evaluated.

To identify the NOS enzymes expressed in the primary fibroblasts used in this study, western blots were performed. It was expected that eNOS and nNOS would be present in the cells expressing these genes, but the expression of iNOS was not predicted since this enzyme is not constitutively expressed. We predicted eNOS expression to correlate with the eNOS gene expression, meaning WT fibroblasts express eNOS and the DKO and enos KO do not. However, the levels of eNOS were inconclusive since each western blot result showed inconsistent levels of eNOS protein, even in the WT cells. The inconsistency found may have been due to antibody issues, protein concentration, actual inconsistency in eNOS expression, or other factors. The expression and activity of eNOS will be evaluated in a subsequent study to provide better understanding. The western blot results for nNOS protein showed signal detection in the WT and eNOS KO/nNOS WT samples in a UV-independent manner, but not in the DKO samples (Figure 14). This indicated that the fibroblasts used that were WT for nNOS did produce this enzyme. This result is important because the literature is contradictory in this regard and there is not full agreement about the expression of nNOS in fibroblasts (Wang et al., 1996). Because the levels were fairly consistent in the control and sUV irradiated samples (Figure 14), we do not believe nNOS to be upregulated in response to sUV. iNOS levels were evaluated to investigate a possible compensation effect by the KO fibroblasts.

Because the DKO and eNOS KO fibroblasts should be lacking cNOS enzymes, we considered that iNOS may be upregulated to compensate for the lower NO· production. The

results showed that iNOS was only detected in the WT fibroblasts, and was not upregulated in the DKO or eNOS KO fibroblasts (Figure 14). This indicates these fibroblasts were not compensating for the constitutive NOS KO. This is important because we can get a better understanding of the role of cNOS after sUV in these fibroblasts knowing that iNOS is not contributing to the KO fibroblasts response at the timepoints used. It has been established that iNOS is not expressed and activated early after UV exposure, which indicates why the signal was not present in the DKO or eNOS KO samples. It was anticipated that iNOS would not have been expressed in any of the fibroblasts since it is induced after stress and we only evaluated early time points. However, in the literature iNOS has been also observed in normal peritoneal and adhesion fibroblast (Jiang et al., 2009). Since iNOS expression is regulated by, among others, NF-κB and oxidative stress (Pautz et al., 2010), we cannot rule out that the levels of NOS present in the WT and eNOS KO samples are enough to induce the expression of iNOS in these cell lines. Further analysis is necessary to get a more definitive answer as to which of these enzymes are present and active in the fibroblasts isolated from SKH1 mice. This can be done by conducting mRNA analyses for these genes and ROS levels measure.

To evaluate the DNA damage in fibroblasts after sUV irradiation, ELISA was performed to detect CPDs. The results showed increased CPDs in WT and KO fibroblasts immediately after sUV exposure. In WT cells, the CPD levels decreased 20 minutes after sUV exposure, and in the KO fibroblasts, the CPD levels continued to increase 20 minutes after sUV exposure. The decrease in CPDs seen in the WT fibroblasts 20 minutes after sUV is thought to indicate the repair of this DNA damage. Due to the fact that the CPDs continued to increase 20 minutes after

sUV in the KO fibroblasts, we believe that the DNA damage was not being repaired and CPDs continued forming in the DNA (Figure 15). This formation of CPDs observed after UV exposure could correspond to “dark CPDs”, which are the CPDs formed indirectly after UV exposure through photosensitization reactions. It has been shown that CPDs can continue being formed long after UV exposure. A particular study found CPDs continued forming in melanocytes for at least 3 hours after UVA exposure (Premi et al., 2015). Because of these trends, it can be deduced that cNOS is playing a role in the repair of CPDs post sUV exposure. The role of cNOS in CPDs repair is not known and will be further studied. We propose that the mechanism could be dependent on NO·. This molecule could impact the activation of DNA damage repair or the recruitment of DNA damage repair complexes, via induction of post-translational modifications (e.g. S-Nitrosylation) of proteins necessary for DNA damage repair. This topic may be expanded upon to better understand how cNOS is responsible for the repair of UV-induced DNA damage.

To evaluate photoaging in fibroblasts post-sUV, western blots were performed to measure MMP levels. MMP1 was increased after sUV exposure in WT and KO cells. Because the protein levels of active MMP1 were similar between WT and KO fibroblasts, we do not believe cNOS is involved in the regulation of its activation (Figure 16). Regarding MMP2, no significant differences were observed between irradiated and control samples, indicating MMP2 was not upregulated by the dose of sUV applied to the fibroblasts. However, there were significant differences in pro- and cleaved MMP2 levels between the WT, DKO, and eNOS KO/nNOS WT samples (Figure 16). The higher levels of cleaved-MMP2 in the eNOS KO/nNOS WT samples suggest higher levels of active MMP2 in these samples, while the greater signal of

pro-MMP2 in DKO indicate higher levels of inactive MMP2. Because of the greater presence of inactive MMP2 in DKO compared to the eNOS KO/nNOS WT, there may be a correlation between cNOS and the processing and activation of MMP2. Since NOS produce NO·, the DKO fibroblasts should have lower NO· production, and lower oxidative stress. With only one cNOS KO in the eNOS KO/nNOS WT cell line, we expect NO· in greater concentration than the DKO, leading to some oxidative stress. This would lead to more active MMP2 compared to DKO MMP2 production. However, this is not observed in the WT cell line, result that suggest that the correct amount of cNOS and/or NO· is required to maintain the correct balance of active and inactive MMP2.

In addition to MMPs role in the generation of photoaging, MMP1 and MMP2 are also known to facilitate tumor growth (Pittayapruek et al., 2016). Collagenases (MMP1) and Gelatinases (MMP2) are especially crucial in the invasive ability of basal cell carcinoma (BCC). In BCC, MMP1 expression is significantly elevated, as it is the primary collagenolytic enzyme in this skin cancer. MMP1 is also important in the initial growth of tumors as it aids in the cleavage of ECM proteins and growth factors. In fibroblasts surrounding BCC, MMP2 degrades the basement membrane of the skin and other cytoskeletal elements allowing for the growth of skin cancer (Pittayapruek et al., 2016). Our results suggest that cNOS could also be contributing to photocarcinogenesis by regulating the activation of MMP2.

To evaluate the inflammatory response in fibroblasts post sUV exposure, ELISAs were performed to measure IL1, IL6, and TNF-α. The levels of TNF-α and IL1 were below the detectable range of the ELISA kits used. This could indicate that these cytokines are not

produced in a significant amount within the early time frame after sUV exposure. If IL1 and TNF-α were re-evaluated in the late phase after sUV exposure, I would expect detection of these cytokines. The ELISA for IL6 showed significantly higher levels in WT compared to DKO and eNOS KO/nNOS WT. Additionally, the control samples had significantly higher levels when compared to their sUV irradiated counterparts. The DKO samples showed the lowest levels of IL6 (Figure 17). Because of the lack of cNOS, we are expecting that these fibroblasts should be producing the lowest levels of NO· of all the cells studied, which would result in lower levels of oxidative stress. With less oxidative stress, lower IL6 levels would be expected, which is what these results indicated (Ansary et al., 2021). However, the levels of IL6 decreased after sUV at the evaluated times, which was unexpected. This may be caused by 1) the inhibited translation described post sUV irradiation or 2) an increased release of proteases post irradiation. The last considering that we did not add protease inhibitors to the cell culture media. These results indicate some role of cNOS in the inflammatory response, specifically IL6 production. As mentioned, it is unclear whether there is a UV-mediated increase, as the cytokines produced could have been degraded and not detected by the ELISA.

The levels of IL6 secreted by the different fibroblast cell lines may have a connection to the NF-kB pathway (nuclear factor kappa light chain enhancer of activated B cells). Previously it was described in the lab that the activity of the NF-κB transcription factor is increased after UV exposure due to cNOS in UV irradiated keratinocytes (Tong &Wu, 2014). This transcription factor is known to regulate inflammation by increasing the expression of pro-inflammatory cytokines, such as IL6. As inflammation progresses, IL6 signaling is responsible for the switch

to a reparative environment. In addition to IL6's pro-inflammatory role, it also has been described as having pro- and anti-tumor activity. Many studies have shown IL6 to connect chronic inflammation with cancer growth due to this pro-tumor activity. IL6 drives tumor initiation and growth by increasing immune suppression and stimulating angiogenesis (Fisher et al., 2014; Mantovani et al., 2008; Naugle et al., 2008). Conversely, the anti-tumor activity of IL6 can be attributed to its ability to increase leukocyte activity and mediate humoral immunity (Fisher et al., 2014). Because of this ability to influence leukocyte activity, IL6 impacts wound healing, and aids in this reparative process.

4.1 Conclusion and Future Directions

The results seen in this *in vitro* study suggest a role of cNOS in CPDs repair, activation of MMP2, and production of IL6. These results are significant because they help us to understand an *in vivo* study conducted in our research lab. The *in vivo* study established that cNOS KO mice developed more skin lesions compared to WT mice when exposed to the sUV source (Figure 18). In addition to the larger skin lesions on the sUV irradiated KO mice, these mice also exhibited greater wrinkling of the skin and erythema, or reddening of the skin (Figure 18).. Then, the results of this thesis suggest that the lesions are more severe in KO mice due to a lack of CPD repair (which is mediated by cNOS), increased MMP2 activation (regulated by cNOS), and decreased IL6 cytokine, which may be exhibiting anti-tumor activity in the WT mice.

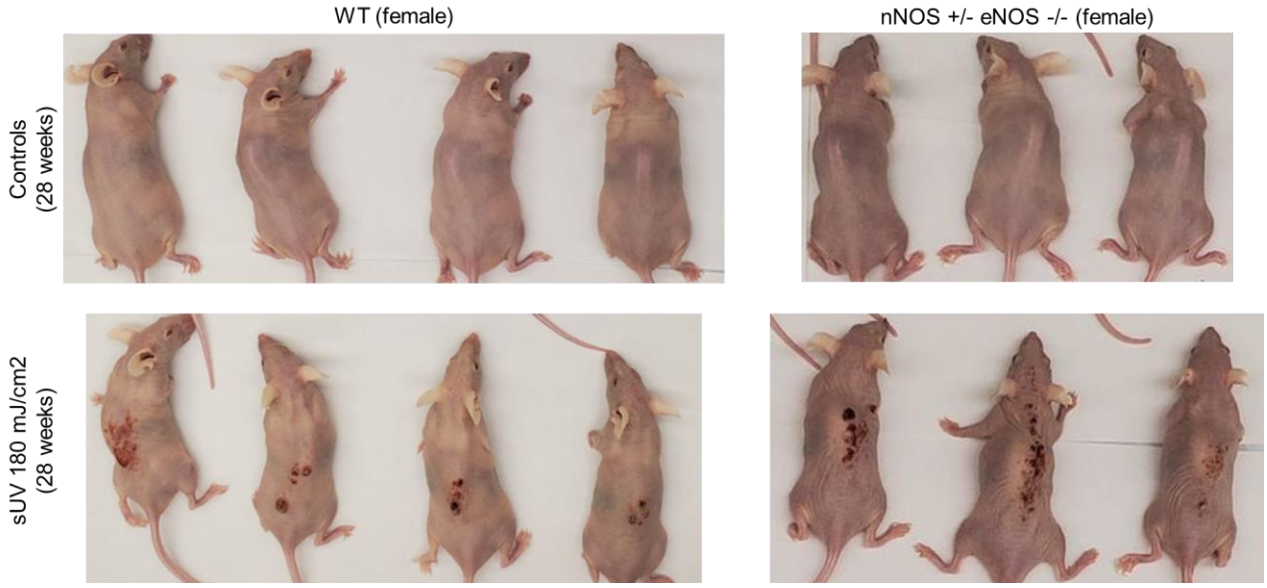

Figure 18 SKH1 hairless mice used in an *in vivo* study of cNOS. The WT mice exposed to sUV have significantly less severe skin lesions compared to the nNOS heterozygote (nNOS +/-) eNOS KO (eNOS -/-) counterparts. The KO mice have also shown signs of increased photoaging and erythema.

This study has many possible future directions and further work is needed to truly understand the role of cNOS in UV-mediated cellular response. To begin, if an *in vitro* approach is to be continued, the primary cell line of fibroblasts would need to be expanded to include all combinations of nNOS and eNOS knockouts. Additionally, cells collected from male and female mice should be used to determine if there is a sex-dependent phenomenon occurring with the fibroblasts, since in the mice model, females and males respond differently. In addition, and to better understand the role of cNOS in DNA repair, CPD formation and repair should continue to be studied. More timepoints could be evaluated to determine if CPDs are being repaired later or not at all. Also, the amount of NO· present before and after sUV exposure should be measured to establish what ideal vs excess NO· levels are. mRNA analysis of cNOS and iNOS enzymes is

necessary because of the inconclusive western blot results for these proteins. To further expand the inflammatory aim of this thesis, ELISAs for inflammatory markers should be repeated and performed with medium from more time points (and later after sUV exposure). In addition, protease inhibitors should be considered in future work to establish if the cytokines are truly not being produced, or if they are being produced and degraded.

The ultimate goal of research in this area of photo-biochemistry would be to identify cNOS as a target for treatment against UV-induced skin damage. Finding new targets for treatment against photo-damage is valuable information to the improvement of health and wellbeing, as well as in the business and industry of skincare. The study of prevention of disease is important to the betterment of health, and given the detrimental effects of UV exposure, studying ways to prevent UV damage is extremely beneficial. The high incidence of skin cancer alludes to the importance of practical, safe, and effective preventive care against UV damage.

Bibliography

2022-cancer-facts-and-figures. (n.d.).

Alkaitis MS, Crabtree MJ. Recoupling the cardiac nitric oxide synthases: tetrahydrobiopterin synthesis and recycling. Curr Heart Fail Rep. 2012 Sep;9(3):200-10. doi: 10.1007/s11897-012-0097-5. PMID: 22711313; PMCID: PMC3406312.

Ahmed, N. U., Ueda, M., Nikaido, O., Osawa, T., & Ichihashi, M. (n.d.). *High levels of 8-hydroxy-2 0-deoxyguanosine appear in normal human epidermis after a single dose of ultraviolet radiation*.

Anderson, R. R., & Parrish, J. A. (1981). The optics of human skin. *The Journal of investigative dermatology*, *77*(1), 13–19. https://doi.org/10.1111/1523-1747.ep12479191

Ansary, T. M., Razib Hossain, M., Kamiya, K., Komine, M., Ohtsuki, M., & Aranda, C. (2021). *Molecular Sciences Inflammatory Molecules Associated with Ultraviolet Radiation-Mediated Skin Aging*. https://doi.org/10.3390/ijms22083974

Bahamondes Lorca, V. A. (2021). *Effect of the Constitutive Nitric Oxide Synthase and Peroxynitrite in DNA Damage and Autophagy Response after UVB Irradiation on Keratinocytes A dissertation presented to*.

Bahamondes Lorca, V. A., McCulloch, M. K., Ávalos-Ovando, Ó., Govorov, A. O., Rahman, F., & Wu, S. (2022). Characterization of UVB and UVA-340 Lamps and Determination of

Their Effects on ER Stress and DNA Damage. *Photochemistry and Photobiology*. https://doi.org/10.1111/php.13585

Bahamondes Lorca, V. A., & Wu, S. (2020). Role of constitutive nitric oxide synthases in the dynamic regulation of the autophagy response of keratinocytes upon UVB exposure. *Photochemical & photobiological sciences : Official journal of the European Photochemistry Association and the European Society for Photobiology*, *19*(11), 1559–1568. https://doi.org/10.1039/d0pp00280

Benavides, F., Oberyszyn, T. M., VanBuskirk, A. M., Reeve, V. E., & Kusewitt, D. F. (2009). The hairless mouse in skin research. *Journal of Dermatological Science*, *53*(1), 10–18. https://doi.org/10.1016/j.jdermsci.2008.08.012

Bernard, J. J., Gallo, R. L., & Krutmann, J. (n.d.). Photoimmunology: how ultraviolet radiation affects the immune system. *Nature Reviews Immunology*. https://doi.org/10.1038/s41577-019-0185-9

Brown, T. M., & Krishnamurthy, K. (2022). Histology, Dermis. In *StatPearls [Internet]*. StatPearls Publishing. https://www.ncbi.nlm.nih.gov/books/NBK535346/

Cadet, J., Mouret, S., Ravanat, J. L., & Douki, T. (2012). Photoinduced damage to cellular DNA: direct and photosensitized reactions. *Photochemistry and photobiology*, *88*(5), 1048–1065. https://doi.org/10.1111/j.1751-1097.2012.01200.x

Cadet, J., Douki, T., & Ravanat, J.-L. (2015). Invited Review Oxidatively Generated Damage to Cellular DNA by UVB and UVA Radiation †, ‡. *Photochemistry and Photobiology*, *91*, 140–155. https://doi.org/10.1111/php.12368

Cals-Grierson, M. M., & Ormerod, A. D. (2004). Nitric oxide function in the skin. *Nitric oxide : biology and chemistry*, *10*(4), 179–193. https://doi.org/10.1016/j.niox.2004.04.005

Chen, K., Pittman, R. N., & Popel, A. S. (2008). Review Nitric Oxide in the Vasculature: Where Does It Come From and Where Does It Go? A Quantitative Perspective. *ANTIOXIDANTS & REDOX SIGNALING*, *10*(7), 1185–1198. https://doi.org/10.1089/ars.2007.1959

Clancy, S. (2008). *Mutation, DNA Repair, and DNA Integrity | Learn Science at Scitable*. https://www.nature.com/scitable/topicpage/dna-damage-repair-mechanisms-for-maintaining-dna-344/

Costa, E. D., Rezende, B. A., Sf, C., & Lemos, V. S. (2016). Neuronal Nitric Oxide Synthase in Vascular Physiology and Diseases. *Front. Physiol*, *7*, 206. https://doi.org/10.3389/fphys.2016.00206\

Czyz, M. (2019). Fibroblast Growth Factor Receptor Signaling in Skin Cancers. *Cells*, *8*(6), 540. https://doi.org/10.3390/cells8060540

de Jager, T. L., Cockrell, A. E., Plessis, S. S. du, Cockrell, • A E, & du Plessis, • S S. (2017). Ultraviolet Light Induced Generation of Reactive Oxygen Species. *Advances in Experimental Medicine and Biology*, *996*. https://doi.org/10.1007/978-3-319-56017-5_2

Deanfield, J. E., Halcox, J. P., & Rabelink, T. J. (2007). Endothelial function and dysfunction: Testing and clinical relevance. In *Circulation* (Vol. 115, Issue 10, pp. 1285–1295). https://doi.org/10.1161/CIRCULATIONAHA.106.652859

D'orazio, J., Jarrett, S., Amaro-Ortiz, A., & Scott, T. (2013). UV Radiation and the Skin. *Int. J. Mol. Sci*, *14*, 12222–12248. https://doi.org/10.3390/ijms140612222

Douki, T., Reynaud-Angelin, A., Cadet, J., & Sage, E. (2003). Bipyrimidine photoproducts rather than oxidative lesions are the main type of DNA damage involved in the genotoxic effect of solar UVA radiation. *Biochemistry*, *42*(30), 9221–9226. https://doi.org/10.1021/bi034593c

Engelsen, O. (2010). The Relationship between Ultraviolet Radiation Exposure and Vitamin D Status. *Nutrients*, *2*, 482–495. https://doi.org/10.3390/nu2050482

Fisher, D. T., Appenheimer, M. M., & Evans, S. S. (2014). The Two Faces of IL-6 in the Tumor Microenvironment. *Seminars in Immunology*, *26*(1), 38–47. https://doi.org/10.1016/j.smim.2014.01.008

Frank, S., Ka¨mpfer, H., Ka¨mpfer, K., Wetzler, C., & Pfeilschifter, J. (2002). Nitric oxide drives skin repair: Novel functions of an established mediator. In *Kidney International* (Vol. 61).

Förstermann, U., & Sessa, W. C. (2012). Nitric oxide synthases: regulation and function. *European heart journal*, *33*(7), 829–837d. https://doi.org/10.1093/eurheartj/ehr304

Goto, N., Bazar, G., Kovacs, Z., Kunisada, M., Morita, H., Kizaki, S., Sugiyama, H., Tsenkova, R., & Nishigori, C. (2015). *Detection of UV-induced cyclobutane pyrimidine dimers by near-infrared spectroscopy and aquaphotomics*. https://doi.org/10.1038/srep11808

Groves, J. T., & Wang, C. C. Y. (2000). Nitric oxide synthase: Models and mechanisms. *Current Opinion in Chemical Biology*, *4*(6), 687–695. https://doi.org/10.1016/S1367-5931(00)00146-0

Gsell, C., Richly, H., Coin, F., & Naegeli, H. (2020). A chromatin scaffold for DNA damage recognition: How histone methyltransferases prime nucleosomes for repair of ultraviolet light-induced lesions. *Nucleic Acids Research*, *48*(4), 1652–1668. https://doi.org/10.1093/nar/gkz1229

Jiang, Z. L., Fletcher, N. M., Diamond, M. P., Abu-Soud, H. M., & Saed, G. M. (2009). Hypoxia regulates iNOS expression in human normal peritoneal and adhesion fibroblasts through nuclear factor kappa B activation mechanism. *Fertility and sterility*, *91*(2), 616–621. https://doi.org/10.1016/j.fertnstert.2007.11.059

Jiang, H. Y., & Wek, R. C. (2005). GCN2 phosphorylation of eIF2alpha activates NF-kappaB in response to UV irradiation. *The Biochemical journal*, *385*(Pt 2), 371–380. https://doi.org/10.1042/BJ20041164

Juzeniene, A., Brekke, P., Dahlback, A., Andersson-Engels, S., Reichrath, J., Moan, K., Holick, M. F., Grant, W. B., & Moan, J. (2011). Solar radiation and human health. *Reports on Progress in Physics*, *74*(6). https://doi.org/10.1088/0034-4885/74/6/066701

Kinner, A., Wu, W., Staudt, C., & Iliakis, G. (2008). Gamma-H2AX in recognition and signaling of DNA double-strand breaks in the context of chromatin. *Nucleic acids research*, *36*(17), 5678–5694. https://doi.org/10.1093/nar/gkn550

Kuhn, A., Fehsel, K., Lehmann, P., Krutmann, J., Ruzicka, T., & Kolb-Bachofen, V. (1998). Aberrant Timing in Epidermal Expression of Inducible Nitric Oxide Synthase After UV Irradiation in Cutaneous Lupus Erythematosus. *Journal of Investigative Dermatology*, *111*(1), 149–153. https://doi.org/10.1046/j.1523-1747.1998.00253.x

Kuo, L. J., & Yang, L. X. (2008). Gamma-H2AX - a novel biomarker for DNA double-strand breaks. *In vivo (Athens, Greece)*, *22*(3), 305–309.

Lago, J. C., & Puzzi, M. B. (2019). The effect of aging in primary human dermal fibroblasts. *PLoS ONE*, *14*(7). https://doi.org/10.1371/journal.pone.0219165

Lans, H., Marteijn, J. A., Schumacher, B., Hoeijmakers, J. H., Jansen, G., & Vermeulen, W. (2010). Involvement of global genome repair, transcription coupled repair, and chromatin remodeling in UV DNA damage response changes during development. *PLoS genetics*, *6*(5), e1000941. https://doi.org/10.1371/journal.pgen.1000941

Lee JW, Ratnakumar K, Hung KF, Rokunohe D, Kawasumi M. Deciphering UV-induced DNA Damage Responses to Prevent and Treat Skin Cancer. Photochem Photobiol. 2020 May;96(3):478-499. doi: 10.1111/php.13245. Epub 2020 May 4. PMID: 32119110; PMCID: PMC7651136.

Leverkus, M., Yaar, M., Eller, M. S., Tang, E. H., & Gilchrest, B. A. (1998). *Post-Transcriptional Regulation of UV Induced TNF-α Expression Ultraviolet (UV) irradiation exerts multiple effects on skin cells, including the induction of several cytokines involved in immunomodulation*.

Li, H., Jamal, J., Plaza, C., Pineda, S. H., Chreifi, G., Jing, Q., Cinelli, M. A., Silverman, R. B., & Poulos, T. L. (2014). Structures of human constitutive nitric oxide synthases. *Research Papers Acta Cryst*, *70*, 2667–2674. https://doi.org/10.1107/S1399004714017064

Liu, W., & Wu, S. (2010). Differential roles of nitric oxide synthases in regulation of ultraviolet B light-induced apoptosis. *Nitric oxide : biology and chemistry*, *23*(3), 199–205. https://doi.org/10.1016/j.niox.2010.06.003

Layers of the Skin | Anatomy and Physiology I. (n.d.). Retrieved April 5, 2023, from https://courses.lumenlearning.com/suny-ap1/chapter/layers-of-the-skin/

Mantovani, A., Allavena, P., Sica, A., & Balkwill, F. (2008). Cancer-related inflammation. *Nature*, *454*(7203), 436–444. https://doi.org/10.1038/nature07205

Mazumder, T., Nath, S., Nath, N. & Kumar, M. (2014). Head and Neck Squamous Cell Carcinoma: Prognosis using molecular approach. *Open Life Sciences*, *9*(6), 593-613. https://doi.org/10.2478/s11535-014-0292-3

Mouret, S., Baudouin, C., Charveron, M., Favier, A., Cadet, J., & Douki, T. (2006). Cyclobutane pyrimidine dimers are predominant DNA lesions in whole human skin exposed to UVA

radiation. *Proceedings of the National Academy of Sciences*, *103*(37), 13765–13770. https://doi.org/10.1073/pnas.0604213103

Murphrey, M. B., Miao, J. H., & Zito, P. M. (2022). Histology, Stratum Corneum. In *StatPearls [Internet]*. StatPearls Publishing. https://www.ncbi.nlm.nih.gov/books/NBK513299/

Naugler, W. E., & Karin, M. (2008). The wolf in sheep's clothing: the role of interleukin-6 in immunity, inflammation and cancer. *Trends in molecular medicine*, *14*(3), 109–119. https://doi.org/10.1016/j.molmed.2007.12.007

Nilforoushzadeh, M. A., Razzaghi, M., Rustamzadeh, A., Zare, S., & Farshi, S. (n.d.). *Effects of Nitric Oxide Activity on the Induction of Oxidative Stress in Skin Cell Signalling, Migration and Apoptosis*. 4.

Oh, K. S., Bustin, M., Mazur, S. J., Appella, E., & Kraemer, K. H. (2011). UV-induced histone H2AX phosphorylation and DNA damage related proteins accumulate and persist in nucleotide excision repair-deficient XP-B cells. *DNA repair*, *10*(1), 5–15. https://doi.org/10.1016/j.dnarep.2010.09.004

Pautz, A., Art, J., Hahn, S., Nowag, S., Voss, C., & Kleinert, H. (2010). Regulation of the expression of inducible nitric oxide synthase. *Nitric Oxide*, *23*(2), 75–93. https://doi.org/10.1016/j.niox.2010.04.007

Pfeifer G. P. (2020). Mechanisms of UV-induced mutations and skin cancer. *Genome instability & disease*, *1*(3), 99–113. https://doi.org/10.1007/s42764-020-00009-8

Pittayapruek, P., Meephansan, J., Prapapan, O., Komine, M., & Ohtsuki, M. (2016). Role of Matrix Metalloproteinases in Photoaging and Photocarcinogenesis. *International Journal of Molecular Sciences*, *17*(6), 868. https://doi.org/10.3390/ijms17060868

Premi, S., Wallisch, S., Mano, C. M., Weiner, A. B., Bacchiocchi, A., Wakamatsu, K., Bechara, E. J. H., Halaban, R., Douki, T., & Brash, D. E. (2015). Chemiexcitation of Melanin Derivatives Induces DNA Photoproducts Long after UV Exposure. *Science (New York, N.Y.)*, *347*(6224), 842–847. https://doi.org/10.1126/science.1256022

Rakoff-Nahoum S. (2006). Why cancer and inflammation? *The Yale journal of biology and medicine*, *79*(3-4), 123–130.

Ramadon, Delly & McCrudden, Maeliosa & Courtenay, Aaron & Donnelly, Ryan. (2021). Enhancement strategies for transdermal drug delivery systems: current trends and applications. Drug Delivery and Translational Research. 12. 10.1007/s13346-021-00909-6.

Ryu, J., Park, S. J., Kim, I. H., Choi, Y. H., & Nam, T. J. (2014). Protective effect of porphyra-334 on UVA-induced photoaging in human skin fibroblasts. *International Journal of Molecular Medicine*, *34*(3), 796–803. https://doi.org/10.3892/ijmm.2014.1815

Sasaki, N., Yamashita, T., Kasahara, K., Fukunaga, A., Yamaguchi, T., Emoto, T., Yodoi, K., Matsumoto, T., Nakajima, K., Kita, T., Takeda, M., Mizoguchi, T., Hayashi, T., Sasaki, Y., Hatakeyama, M., Taguchi, K., Washio, K., Sakaguchi, S., Malissen, B., … Hirata, K. I. (2017). UVB exposure prevents atherosclerosis by regulating immunoinflammatory

responses. *Arteriosclerosis, Thrombosis, and Vascular Biology*, *37*(1), 66–74. https://doi.org/10.1161/ATVBAHA.116.308063

Schuch, A. P., Moreno, N. C., Schuch, N. J., Martins Menck, C. F., & Machado Garcia, C. C. (2007). Sunlight damage to cellular DNA: Focus on oxidatively generated lesions. *Free Radical Biology and Medicine*, *107*, 110–124. https://doi.org/10.1016/j

Skin: Layers, Structure and Function. (n.d.). Cleveland Clinic. Retrieved April 5, 2023, from https://my.clevelandclinic.org/health/articles/10978-skin

Sorrell, J. M., & Caplan, A. I. (2004). Fibroblast heterogeneity: more than skin deep. *Journal of cell science*, *117*(Pt 5), 667–675. https://doi.org/10.1242/jcs.01005

Svobodova, A., Walterova, D., & Vostalova, J. (2006). Ultraviolet light induced alteration to the skin. *Biomedical papers of the Medical Faculty of the University Palacky, Olomouc, Czechoslovakia*, *150*(1), 25–38. https://doi.org/10.5507/bp.2006.003

Tong, L., & Wu, S. (2014). The role of constitutive nitric-oxide synthase in ultraviolet B light-induced nuclear factor κB activity. *Journal of Biological Chemistry*, *289*(38), 26658–26668. https://doi.org/10.1074/jbc.M114.600023

Tracy, L. E., Minasian, R. A., & Caterson, E. J. (2016). Extracellular Matrix and Dermal Fibroblast Function in the Healing Wound. *Advances in wound care*, *5*(3), 119–136. https://doi.org/10.1089/wound.2014.0561

Valacchi, G., Sticozzi, C., Pecorelli, A., Cervellati, F., Cervellati, C., & Maioli, E. (n.d.). Cutaneous responses to environmental stressors. *Ann. N.Y. Acad. Sci*. https://doi.org/10.1111/j.1749-6632.2012.06724.x

Walmacq, C., Cheung, A. C. M., Kireeva, M. L., Lubkowska, L., Ye, C., Gotte, D., Strathern, J. N., Carell, T., Cramer, P., & Kashlev, M. (2012). Mechanism of Translesion Transcription by RNA Polymerase II and Its Role in Cellular Resistance to DNA Damage. *Molecular Cell*, *46*(1), 18–29. https://doi.org/10.1016/J.MOLCEL.2012.02.006

Walmsley, G. G., Maan, Z. N., Hu, M. S., Atashroo, D. A., Whittam, A. J., Duscher, D., Tevlin, R., Marecic, O., Lorenz, H. P., Gurtner, G. C., Longaker, M. T. Murine Dermal Fibroblast Isolation by FACS. J. Vis. Exp. (107), e53430, doi:10.3791/53430 (2016).

Wu, S., Wang, L., Jacoby, A. M., Jasinski, K., Kubant, R., & Malinski, T. (2009). *Ultraviolet B Light-induced Nitric Oxide / Peroxynitrite Imbalance in Keratinocytes-Implications for Apoptosis and Necrosis*. https://doi.org/10.1111

Xia L, Tan S, Zhou Y, Lin J, Wang H, Oyang L, Tian Y, Liu L, Su M, Wang H, Cao D, Liao Q. Role of the NFκB-signaling pathway in cancer. Onco Targets Ther. 2018 Apr 11;11:2063-2073. doi: 10.2147/OTT.S161109. PMID: 29695914; PMCID: PMC5905465.

Yamaba, H., Haba, M., Kunita, M., Sakaida, T., Tanaka, H., Yashiro, Y., & Nakata, S. (2016). *Morphological change of skin fibroblasts induced by UV Irradiation is involved in photoaging*. https://doi.org/10.1111/exd.13084

Yousef, H., Alhajj, M., & Sharma, S. (2022). Anatomy, Skin (Integument), Epidermis. In StatPearls. StatPearls Publishing.

Zhou, Y. (2022, September). Identification of Factors in IKKα Promoter After UVB [Poster] 41st American Society for Photobiology Biennial Meeting, Albuquerque, NM.